Spring 2023

Thermal Stability of Platinum-Silicon Alloy Films Grown on Langasite Substrates for use in Microwave Acoustic Sensor Technology

Kell Fremouw
University of Maine - Main, kell.fremouw@maine.edu

THERMAL STABILITY OF PLATINUM-SILICON ALLOY FILMS GROWN ON LANGASITE SUBSTRATES FOR USE IN MICROWAVE ACOUSTIC SENSOR TECHNOLOGY

by

Kell Fremouw

A Thesis Submitted in Partial Fulfillment
of the Requirements for a Degree with Honors
(Engineering Physics)

The Honors College

University of Maine

May 2023

Advisory Committee:

Dr. Robert J. Lad, Professor of Physics, Member of FIRST, Advisor
Dr. Carl P. Tripp, Professor of Chemistry, Member of FIRST
Dr. Jordan LaBouff, Associate Professor of Psychology and Honors
Dr. Samuel T. Hess, Professor of Physics / Cooperating Professor of Chemistry

ABSTRACT

Wireless sensors that can operate in temperatures up to 1000°C are widely needed for real time monitoring of large-scale industrial processes. Such sensors will improve efficiency and prevent component failure. Under previous work at UMaine, Surface Acoustic Wave Resonator (SAWR) sensors fabricated on piezoelectric langasite ($La_3Ga_5SiO_{14}$) wafers have shown promise for wireless strain measurements at high temperatures. However, there is a major technical challenge in attaching SAWR langasite based sensors to metal parts because the large differences in the coefficient of thermal expansion (CTE) between langasite and metals leads to large thermal stresses and fracture of the associated materials during thermal cycling. Preliminary work resulted in the development of a multilayered adhesive containing graded CTE values using platinum, silicon, zirconium, and copper which showed promising adhesion between langasite and steel. However, problems with the multilayered adhesive include non-uniform bonding leading to irreproducible behavior, film delamination, weakening through oxidation, and lack of thermal stability. This thesis reports on results of experiments performed using facilities in UMaine's Frontier Institute for Research in Sensor Technologies (FIRST). The thermal stability of Pt_xSi_{1-x} alloy films deposited on langasite substrates was investigated to create a uniform, reproducible layer to reliably adhere langasite to a copper overlayer. The Pt_xSi_{1-x} films were deposited to a thickness of ~150nm using an electron beam evaporation technique carried out in ultra-high vacuum. Several Pt_xSi_{1-x} films were synthesized by co-deposition from elemental Si and Pt sources and then subjected to annealing treatments up to 850°C in vacuum, air, or N_2 process gases. The PtSi alloy composition was identified to be the most promising for creating a

uniform, thermally stable film as determined from X-ray diffraction and scanning electron microscopy analysis. A 500 nm thick copper layer deposited on a PtSi film using a sputter deposition technique yielded a thermally stable film configuration due to a chemical reaction across the PtSi/Cu interface.

ACKNOWLEDGEMENTS

I would like to thank my advisor for this project Dr. Robert Lad (Prof, UMaine, FIRST) and Luke Doucette (Research Scientist, FIRST) for their assistance guiding my research, Michael Call (Research Engineer, FIRST) for help with thin film deposition, and Emma Perry (CORE, UMaine) and Dr. Morton Greenslit (FIRST Researcher) for training on materials characterization methods. This work was supported as part of a multi-investigator U.S. Department of Energy EPSCoR grant (DE-SC0021981). I am grateful to have had an opportunity to use facilities and interact with other researchers at the Frontier Institute for Research in Sensor Technologies (FIRST).

TABLE OF CONTENTS

LIST OF FIGURES

1. PROJECT MOTIVATION

In recent years, much attention has been devoted to high temperature (>300°C) sensing. Devices that can operate above 300°C are sought after for use in industrial settings [1]. One of the main applications is in power plants, which are forced to shut down periodically for safety measurements, costing thousands of dollars per hour. In-situ strain gauges could provide continuous monitoring, reducing the need to shut down operation. Uses for in-situ strain sensing also appear in the aerospace industry for monitoring of turbine engines during operation. Commercially available wired strain gauges can work in operation up to 1300°C, and wireless optical sensors up to 1000°C [2]. Wired strain gauges, however, are difficult to install in hard-to-reach areas and cannot measure rotating parts during operation. Dust buildup in the air and contamination on the surface of parts being measured can affect the performance of optical sensors. A new wireless sensor would therefore be a useful addition to the set of high temperature sensing technology.

Under previous work carried out at FIRST, Surface Acoustic Wave Resonator (SAWR) strain sensors have been proposed as alternative high temperature sensors [2]. SAWR devices have the advantage of being able to work wirelessly and without the use of batteries so that they can be set up in difficult to reach places and left to operate without constant maintenance [3]. SAWR sensors are electronic circuits built on top of langasite (LGS) due to its piezoelectric properties. As sound waves move across the surface of the langasite, the piezoelectric nature causes electrical signals to be produced which are picked up by the circuit. As the langasite is strained, the crystal is deformed and the signals change in frequency, thus measuring the strain. SAWR strain sensors

have been successfully implemented in rotating turbine engines producing up to 53,000 g's of force [4].

The difficulty in implementing SAWR sensors in high temperature operations comes from the difference in Coefficient of Thermal Expansion (CTE) between the langasite and metal parts. The CTE is a material property describing how much the material will expand when heated or contract when cooled. The equation $\Delta L = \alpha * L_0 * T$ where α is the CTE, T is temperature, and L_0 is the initial length describes the change in length of a material when subjected to a temperature change. When thermally cycled, 304 stainless steel, which has a CTE of 18 $\frac{\mu m}{m℃}$, expands over three times as much as langasite which has a CTE of 4-5.6 $\frac{\mu m}{m℃}$ [5]. This puts a large amount of stress on any adhesive used because the top of the adhesive which is attached to steel would need to be able to stretch over three times the amount that the bottom, attached to langasite, would stretch as shown in Figure 1.

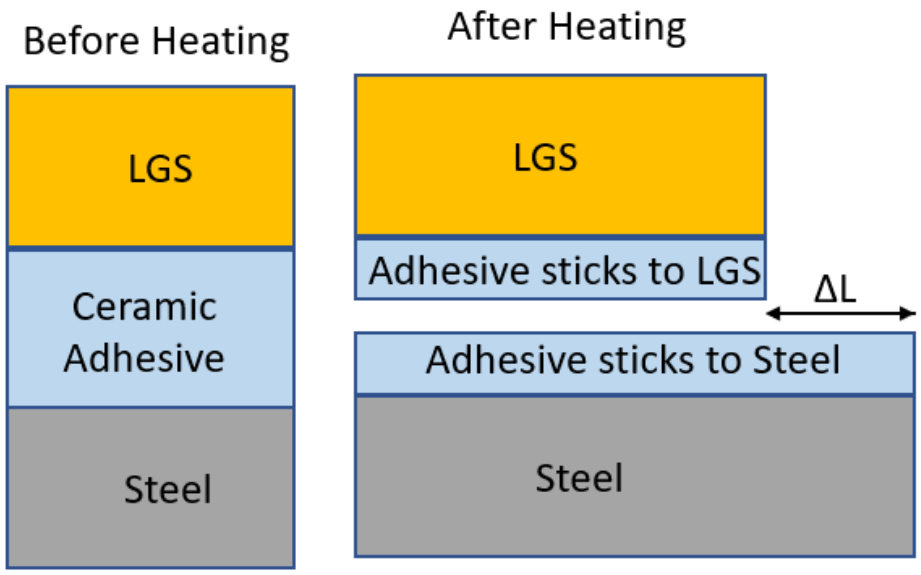

Figure 1. CTE-induced expansion of LGS and steel causes large length difference in adhesive resulting in delamination or cracking.

Under repeated thermal cycling, the thermal stresses fatigue the adhesive over time which damages the adhesive and dampens the sensor's signal. The sensor needs strain to be transmitted through the adhesive, but after thermal cycling the cracks forming or the adhesive softening and becoming more fluid-like reduces the amount of strain transmitted to the sensor. The adhesives also can fully fracture due to the thermal stresses, breaking the connection between the sensor and the part that needs measuring. Composing a multilayered adhesive with each layer having a CTE similar to the layers around it reduces stress in the adhesive layer and allows for successful attachment of langasite to steel. The use of metal layers reduces stress-induced cracking because metals can stretch elastically before permanently deforming and have high fracture strengths. Metals, however, have melting points high enough that the annealing treatment to form the adhesion layer would damage the langasite-based SAWR sensor because langasite melts at 1480°C [3]. Using alloys which melt at lower temperatures than each individual element to reduce the annealing temperature is necessary to create a working adhesive.

CTE differences also cause problems in semiconductor packaging by breaking connections to wires and electrodes [6]. Creating a gradient of CTE values by placing a modulating layer between two connections has been shown to drastically improve the lifetime of power devices [7]. Exploring ways to create CTE graded adhesives, therefore, not only is useful specifically for SAWR sensor attachment, but also has applications throughout the microengineering and packaging industry.

In the summer of 2022, as a precursor to this work, adhesives consisting of bulk (>8μm thick) Cu, Si, Pt, and Zr foils were used to attach langasite to steel [8]. Cu, Si, Pt, and Zr were chosen due to their high temperature mechanical properties, their CTE

values, and potential to melt at low temperatures through alloying with each other [8], [9]. Samples consisting of a langasite crystal attached to a 304-steel substrate with different interfacial multilayer configurations were fabricated and thermally processed in a high temperature furnace up to 950°C under N_2 purge. After heating, cross-sectional samples were prepared by creating a fracture across the interface and X-ray fluorescence experiments were performed in a scanning electron microscope (SEM) to analyze the chemical composition across the adhesive interface. A combination of Zr, Pt, Si thin film layers (< 3.5 micrometers) and Pt, Si, Cu thin foils (<40 micrometers) were investigated under different configurations. Adhesion was achieved between steel and langasite with the strongest configuration involving a 40-micrometer copper foil, 10 micrometer platinum foil, 3.1 micrometer silicon film, and 0.5 micrometer zirconium film. SEM images, like the one shown in Figure 2, show that the Pt-Si layer was the one failing. It was difficult to determine why this layer was failing because every experiment was different, and each section of the sample was different.

Air gaps between the thick foils and lack of consistent elemental concentration led to X-ray diffraction peaks (see Figure 3) showing a variety of unidentified peaks along with PtSi and langasite peaks. There was no consistent crystal structure because the entire sample was melting into alloys with unknown element compositions varying throughout the sample. The langasite surface used has no XRD peaks, so the presence of langasite peaks indicates that the langasite surface cracked, allowing different orientations to interact with the X-rays. The non-uniform bonding shown in Figure 4 and variation in experiments shows that only some of the sample was stuck together. With only a few

contact points for adhesion the samples were failing partially due to lack of consistent bonding.

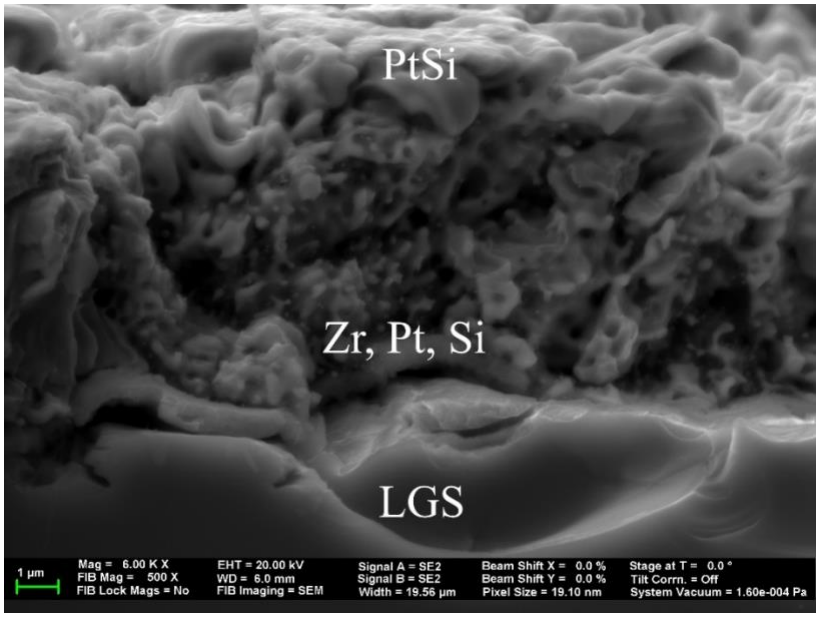

Figure 2. Cross sectional SEM image of fractured adhesive showing layers of Pt/Si and Zr/Pt/Si stuck to LGS.

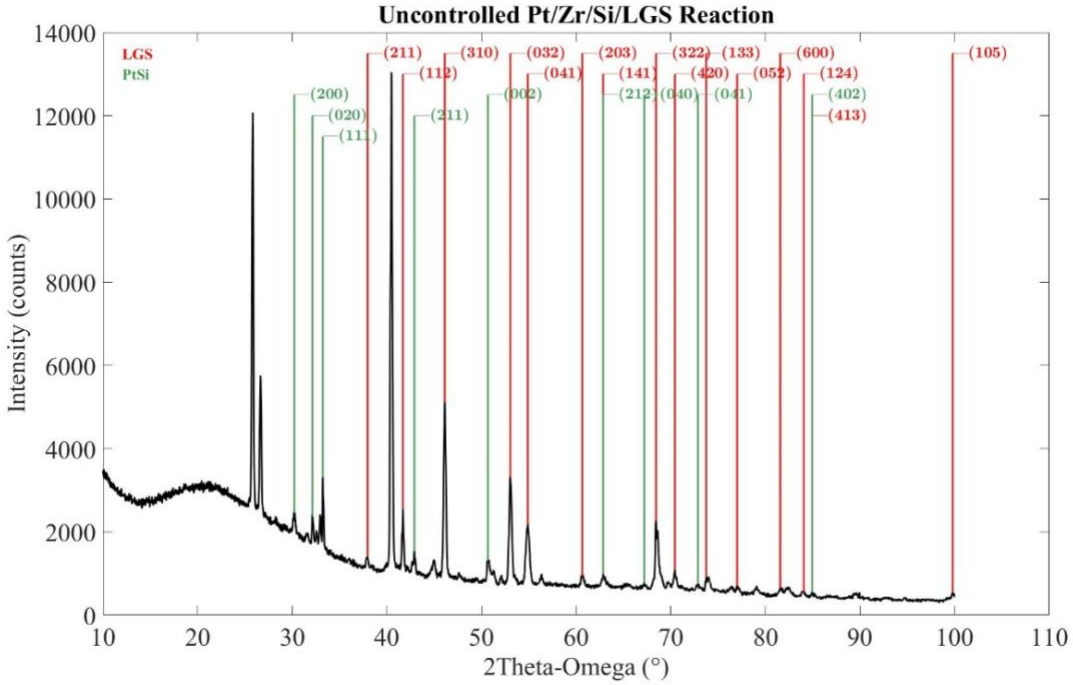

Figure 3. XRD scan of fractured adhesive showing unidentified Pt, Si, Zr, and Cu reaction along with PtSi (0.1° error) and LGS (0.08° error) peaks. Peaks are labeled for specific crystal Miller planes. The error corresponds to the average difference in position between measured peaks and known peak positions calculated from reference data PDF (04-003-0990), (04-016-1898) [33].

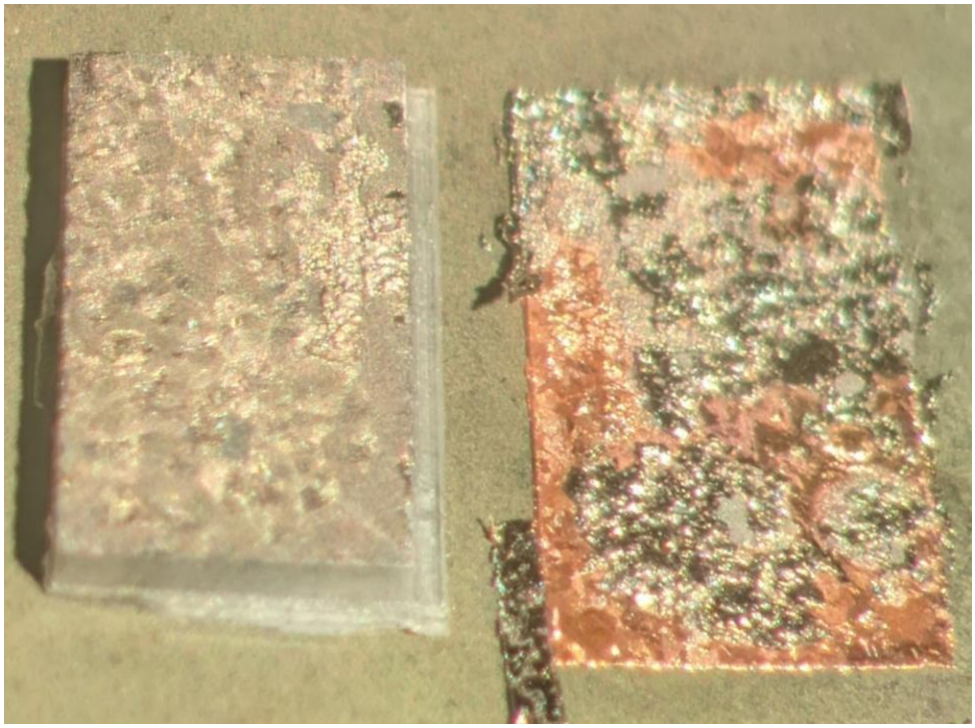

Figure 4. LGS side (left) and Steel side (right) of fractured Cu/Pt/Si/Zr adhesive multilayer sandwich showing evidence of non-uniform bonding.

The aim of this thesis project was to investigate a carefully grown, well defined Pt_xSi_{1-x} thin film layer, attach it to LGS using a Zirconium thin film layer, and explore its overall thermal stability. Measurements of coefficient of thermal expansion changes with alloy composition and film thickness were originally proposed, however, a failure of the XRD high temperature sample stage midway through the project changed the focus to be on thermal stability of such films instead. Carefully controlling the alloy composition by depositing Pt_xSi_{1-x} films a few atomic layers at a time (0.3Å/s) should improve the uniformity, allow for repeatable experiments, and aid in finding the alloy composition and annealing conditions leading to the most thermally stable film. The adhesive is meant to consistently attach langasite samples to various industrial parts thus a reliable, consistent product is necessary. Non-uniformity in the sample (such as a Pt_2Si phase being present in a PtSi sample) could cause non-uniform expansion and contraction when

thermally cycled. Non-uniform expansion and contraction then causes cracking or delamination of the adhesive. Zirconium was included because a thin 10nm Zr layer has been shown to improve the adhesion of platinum electrodes on sapphire [10]. The Zirconium reacts with oxygen present within the langasite which leads to interdiffusion, increasing the adhesion strength [11]. Refining the Pt_xSi_{1-x} layer, attached to LGS using Zr, will increase the effectiveness of the adhesive because the Pt_xSi_{1-x} layer is the point of failure. This work can also be used in other applications of high temperature bonding to langasite or other ceramics as well as the microelectronics and packaging industry.

2. BACKGROUND INFORMATION

Platinum-silicon alloys have been used in high temperature applications for many years. Most research has been focused on how stable the high electrical conductivity of platinum silicide is at high temperatures or how changing the stoichiometry affects the conductivity [12], [13]. Platinum silicide is used throughout the microelectronics industry and films are typically grown via solid state reaction [14]. Studies of how annealing conditions and orientation of substrates affect the silicide grown using solid state reaction have been performed and research is still being done in this area [15]. In recent years, however, co-depositing platinum-silicon alloys has been introduced as an alternative method which can increase the thermal stability [16]. Co-deposited PtSi (platinum and silicon deposited in a 1:1 ratio) was shown to be stable when heated in vacuum to 1000°C with no signs of platinum agglomeration or morphological changes. Solid state reacted PtSi films have varying levels of success but can agglomerate at temperatures as low as 850°C in vacuum, significantly lower than the co-deposited films [16]. Out of PtSi, Pt_2Si and Pt_3Si, PtSi has been identified to have the best thermal stability in air with respect to morphological changes and platinum agglomeration [16], [17].

Building on this past work, this thesis project focused on exploring the thermal stability of platinum-silicon films co-deposited on langasite. Platinum-silicon films are typically grown on sapphire or silicon and the orientation of the film can depend on substrate orientation. At high temperatures, the platinum-silicon thin films may react differently with the langasite substrate than sapphire or silicon. Heat treatments in air, nitrogen, and under vacuum were used to evaluate the thermal stability in a variety of different atmospheres. Additionally, instead of using primarily Scanning Electron

Microscopy (SEM) to detect surface morphology changes or conductivity measurements, X-Ray Diffraction (XRD) was the main technique used. XRD was used to detect changes to the crystal structure of films upon heating as well as change in average grain size. This work also explored the $Pt_{25}Si_7$ eutectic phase which has not been researched before.

In the platinum-silicon phase diagram (refer to Figure 15 on page 23) there is a eutectic point at approximately 78% platinum and 22% silicon [18]. This eutectic melts at a much lower temperature (approximately 851°C) than the rest of the platinum-silicon system which could be beneficial for reducing the expansion and contraction caused by differences in the Coefficient of Thermal Expansion (CTE) upon annealing. To form the most thermally stable platinum-silicon layer, initial heat treatments were done in nitrogen or under vacuum. When platinum-silicon films are heated first in oxygen (i.e. air), silicon will react and form SiO_2 along with a pure platinum coating [19]. When heated first in nitrogen, however, heating up to 600°C in oxygen simply forms a thin SiO_2 layer with silicon that is present at the surface. This oxide could even be prevented in the adhesive if a copper layer protecting the platinum-silicon is used.

One main problem with the platinum-silicon system that has been identified is platinum agglomeration at high temperatures. Thin films typically grow with certain grains forming like pillars on the substrate. Between these grains at the grain boundaries, platinum can accumulate, and once started, more platinum joins until pockets of pure platinum have formed on the surface of the material [20], [21]. The boundaries provide pathways for platinum to travel through. Unstable platinum-silicon films, upon heating, show signs of grain size increasing leading to larger gaps between grains which provide areas for platinum to agglomerate [13]. This agglomeration causes non-uniformity as well

as lack of consistency across experiments. Each layer is different and will change every time it is heated. This is unacceptable when working to create a stable, consistent platinum-silicon layer to be used in a multilayered adhesive. Agglomeration can be reduced using specific alloys and annealing conditions and receives particular attention in this thesis.

The interaction between platinum, silicon, and copper is also of importance because copper is the next layer of the adhesive [8]. When 160nm PtSi films are grown on silicon, the copper diffuses through the PtSi films to form Cu_3Si with the bulk silicon. The PtSi part is stable up to 350°C with no detected reaction with copper [22]. When heating to 400°C, however, copper does interact with PtSi layers to form copper silicide [23]. With the goal of a multilayered adhesive, a silicon layer on top of the PtSi may become necessary to prevent the copper layer from destroying the thin PtSi layer. However, the Cu/PtSi interaction may be helpful in forming a stable, uniform layer.

3. EXPERIMENTAL METHODS

3.1 Deposition of Pt_xSi_{1-x} Thin Film Samples

Langasite (LGS) wafers were acquired with one side polished to an epitaxial grade surface finish with root mean square surface roughness less than one nanometer. The LGS wafers were then diced into 10mm-by-10mm square pieces. When ready to be put in the vacuum chamber, the LGS was first cleaned in an acetone solution and sonicated for 5 minutes, sonicated in isopropanol for 5 minutes, then rinsed with methanol and DI water. Samples were dried by flowing nitrogen gas across the sample. Tantalum plates were sanded, wiped with acetone, and tantalum wires also wiped with acetone were used to hold down the LGS on the tantalum plates. The LGS pieces on tantalum plates were then placed in a vacuum chamber with base pressure of $< 5*10^{-9}$ Torr.

Electron-beam evaporation of individual Pt and Si sources was used to deposit the Pt_xSi_{1-x} films. The rate of deposition of the Pt and Si atoms was between 0.1 angstroms (0.01nm) per second and 0.4 angstroms (0.04nm) per second. The schematic in Figure 5 shows how electron beam evaporation operates and the photograph in Figure 6 shows the setup used. An electron gun creates a stream of electrons which are bent by the Lorentz force from a magnetic field to hit a crucible filled with high-purity silicon, zirconium, or platinum pellets. The material then evaporates (either via sublimation or melting) so that Si, Pt, or Zr atoms impinge upon the sample. By controlling the electron beam current, the rate of deposition can be precisely controlled. The system used has individual shutters for each electron gun. This allows for growing multilayered films with each layer being a

single material, such as the LGS / 5nm Pt / 5nm Si / 5nm Pt sample configuration used in this study.

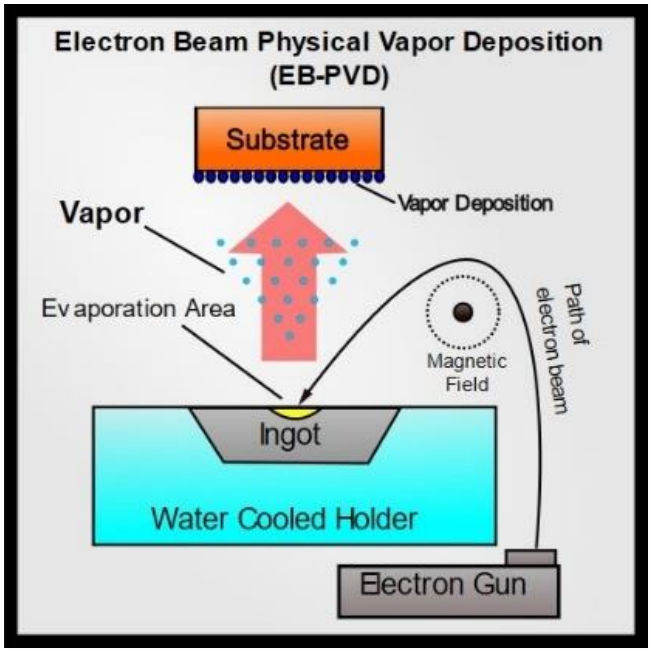

Figure 5. Schematic showing how Pt, Si, or Zr atoms are evaporated using electron beam impingement into a crucible, resulting a highly controlled flux of atoms deposited on the substrate.

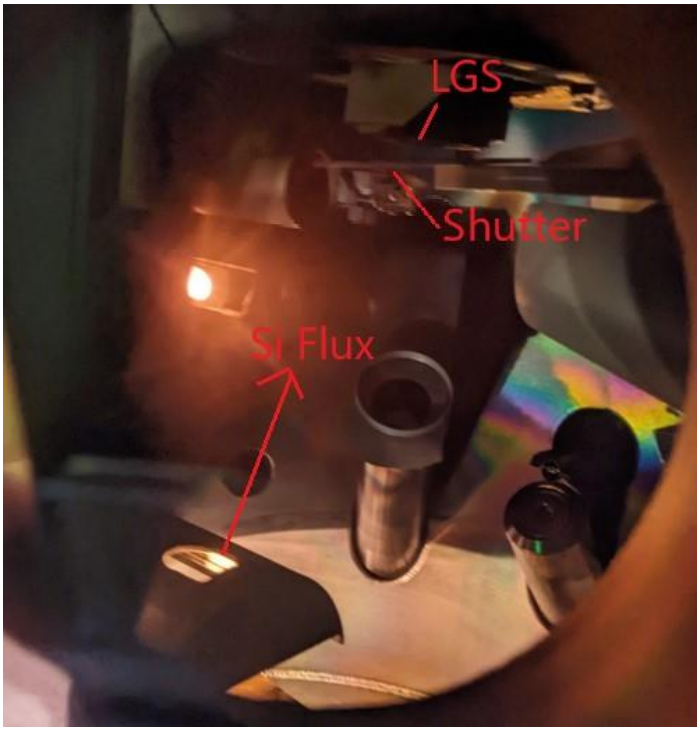

Figure 6. Photograph of EBPVD system used in experiments.

EBPVD allows for very consistent, careful depositions due to the extremely low and precise deposition rates. The rates can be adjusted to form a specific alloy such as PtSi or $Pt_{25}Si_7$ consistently with a low level of error (<3% using thickness measurements and <5% using XPS). Growing samples at high temperatures gives the Pt and Si atoms enough diffusional energy on the film growth surface so that large PtSi crystalline grains can form during the film deposition without annealing afterwards. Using EBPVD, very uniform layers of any elemental composition can be formed. Depositing monolayers carefully using EBPVD under vacuum reduces sample variation by reducing outside variables such as oxidation, and gaps between layers.

An important note about EBPVD is that early samples (before 02_16) were grown with an old batch of silicon which had unsteady deposition rates. The rate used was typically an average of 0.3Å/s but would vary approximately every 1/3 second between any number of values such as 0, 0.1, 0.2, 0.25, 0.35, 0.37Å/s. Samples grown on 02_16 and 03_16 were deposited using a new batch of silicon which had a steadier rate, varying between 0.26Å/s and 0.34Å/s approximately every second.

3.2 Chemical Composition Analysis using X-ray Photoelectron Spectroscopy

X-ray photoelectron spectroscopy is a technique used to determine the elemental composition at the surface of a sample. The XPS system used is attached to the same vacuum system as the EBPVD system. XPS, therefore, was done on samples directly after deposition without the samples leaving vacuum. This allowed for the examination of true surface composition without any oxygen exposure. XPS is a technique where x-rays with specific energies are focused on the sample and the energy of the electrons given off by the sample is measured [24]. The equation used is $KE = h\nu - BE - \phi$ where KE is

the measured kinetic energy of the electron, $h\nu$ is the energy of the x-ray, BE is the binding energy of the electron, and ϕ is the work function of the spectrometer that can be calibrated for each XPS system. The intensity (number of measured electrons) vs. the binding energy is then plotted. The peaks can be matched to known binding energies of different elements. Figure 7 shows an XPS spectrum from a pure platinum film with each of the peaks labeled. This technique is used to find the average elemental composition at the surface of a sample once the relative sensitivity factors for photoemission of each element is known.

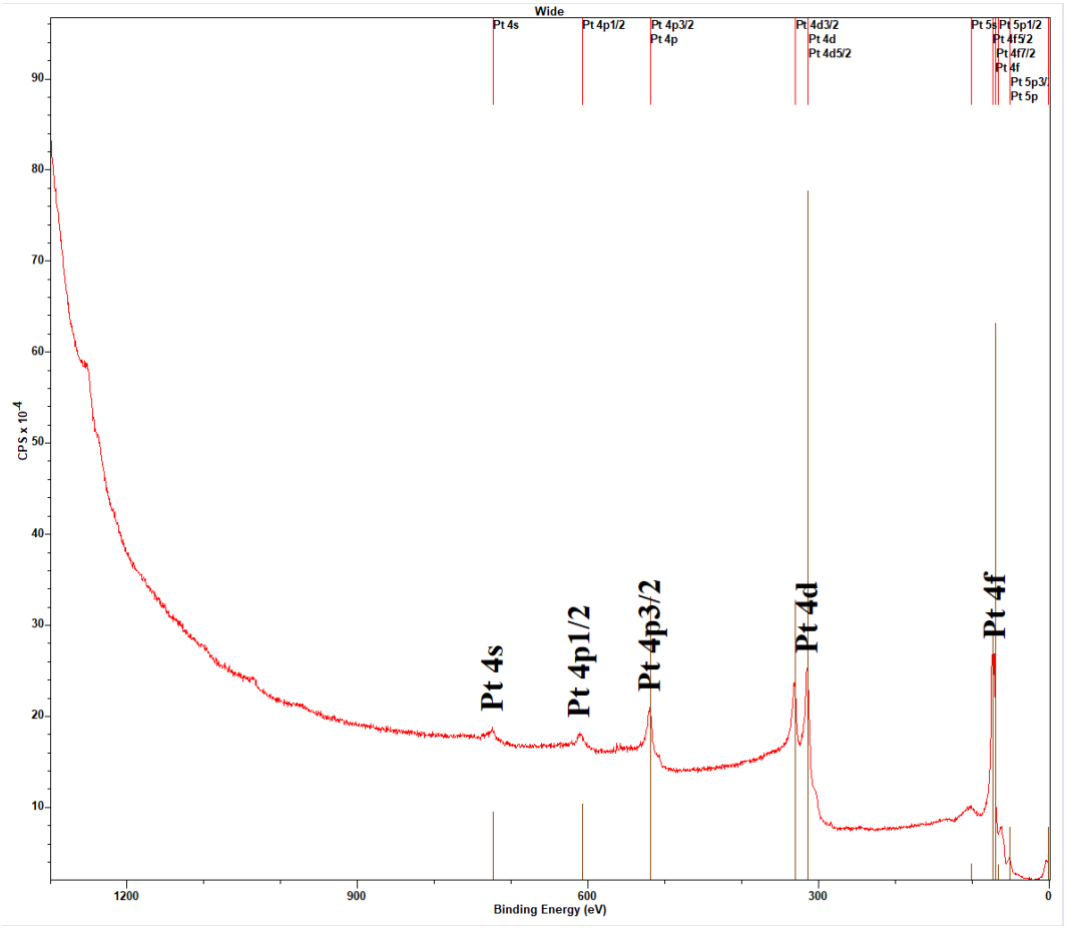

Figure 7. XPS spectrum from 150 nm thick Pt film grown on a LGS substrate.

3.3 Analysis of Crystal Structure using X-Ray Diffraction

X-ray diffraction is a materials characterization technique used to determine the crystal structure of a sample. In the system used, X-rays are generated using Cu-Ka x-rays with a wavelength of 1.54Å. When the x-rays hit the sample, they can be reflected by the atomic planes of atoms. Figure 8 shows a representation of how x-rays reflect when hitting atomic planes. When the distance between planes causes the penetrating x-rays to travel an integer number of wavelengths, the x-rays interfere constructively, causing a peak in the intensity of the detected x-rays. This phenomenon is governed by Bragg's law $n\lambda = 2d_{hkl}\sin(\theta)$ where n is any integer from 1 to infinity, λ is the x-ray wavelength (1.54Å), d_{hkl} is the distance between specific panes (shown in Figure 8) and 2θ is the angle of reflection as defined in Figure 8. The Miller indices h, k, and l, and are used to describe each crystal plane, and the unique distances between planes are used to identify different crystal planes in a given crystal structure.

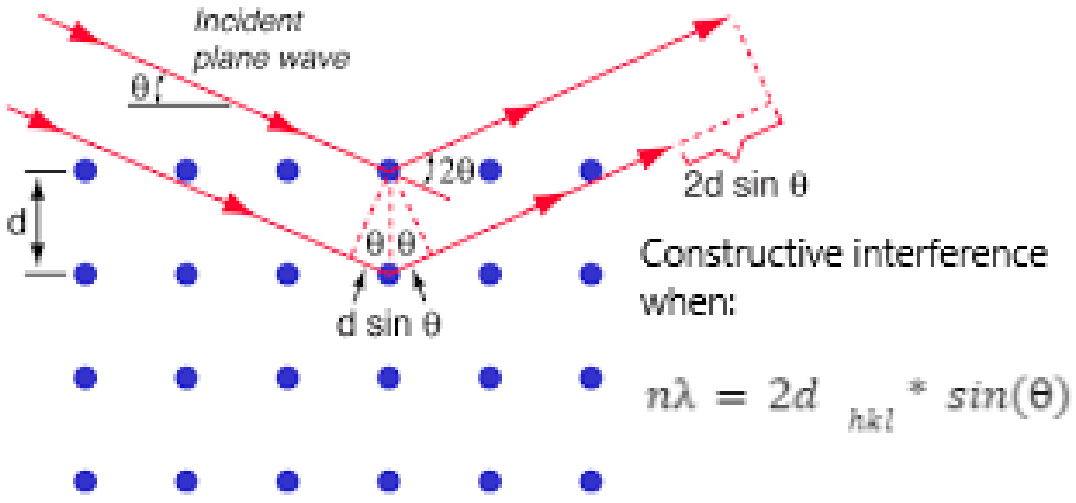

Figure 8. Depiction of X-rays reflecting off crystal planes parallel to the surface leading to Bragg's law: $n\lambda = 2d_{hkl}\sin(\theta)$.

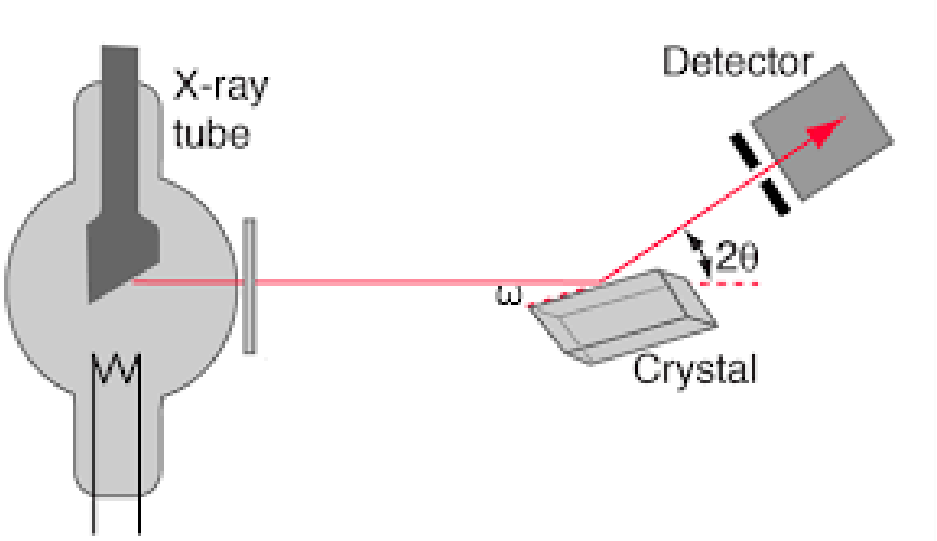

Figure 9. Schematic of XRD experimental set-up showing how the angles ω and 2θ are defined.

Figure 9 shows a schematic of the XRD measurement configuration. During normal 2θ scans, which are the most common scans shown in this work, ω is set equal to θ as shown in Figure 9. During 2θ scans, planes parallel to the surface can meet the conditions of diffraction when $n\lambda = 2d_{hkl}\sin(\theta)$. Planes that are not parallel to the surface, however, are not detected because they reflect the x-rays to a different angle where the detector is not positioned. Figure 10 shows why planes that are not parallel to the surface are not detected during 2θ scans.

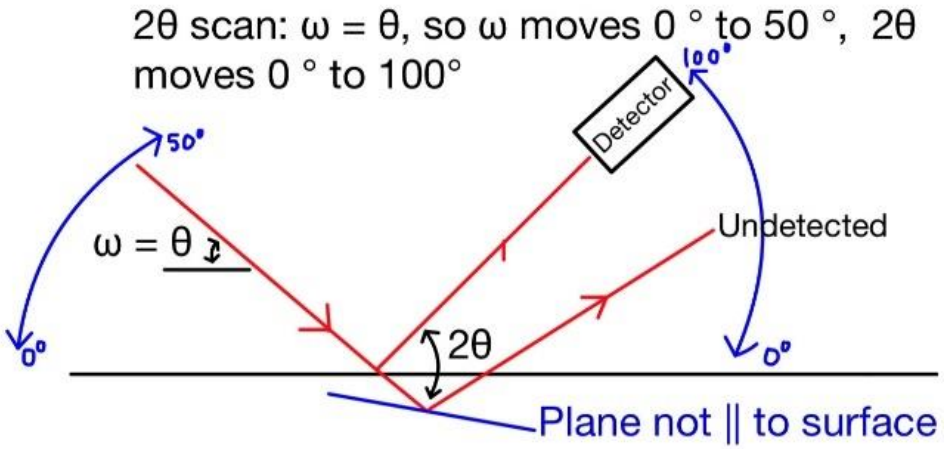

Figure 10. Depiction of 2θ XRD detection of only planes parallel to the surface of the material.

During Grazing Incidence (GI) scans, the ω angle is fixed but the detector moves across 2θ as shown in Figure 11, which allows for the detection of x-rays diffracting off planes not parallel to the surface. The grazing incidence scans are used to determine the in-plane orientation of a crystal. If the crystal grains grow randomly, the different crystal planes will all be parallel to the surface somewhere and be seen in a 2θ scan. If the crystal is growing with a specific plane oriented parallel to the surface, that plane will be very intense in the 2θ scan while other peaks should have low intensities or be undetected. For samples with few peaks in the 2θ scan, grazing incidence scans can be used to check if the crystal is growing in a specific in-plane oriented direction. Figure 12 shows a depiction of GI-XRD geometry. The χ (chi) can be theoretically calculated because PtSi alloys have a known crystal structure. The χ values for various planes can be calculated assuming the film is grown in a certain direction. If, at the correct α, those peaks are shown on the GI-XRD scan, it means that the film is growing in that direction.

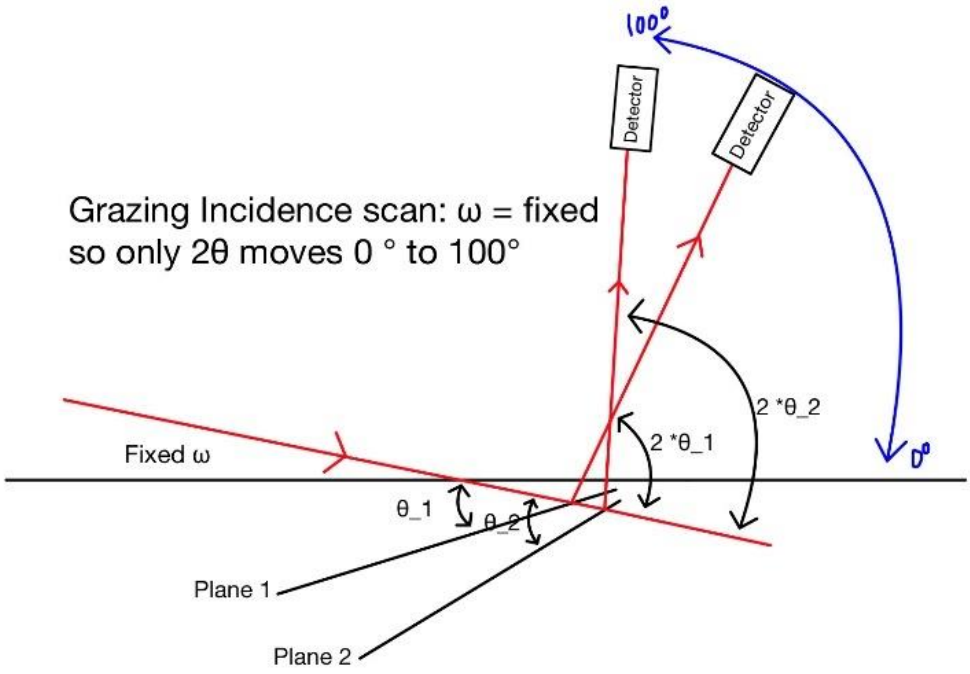

Figure 11. Depiction of GI-XRD scan detecting planes not parallel to the surface of the material.

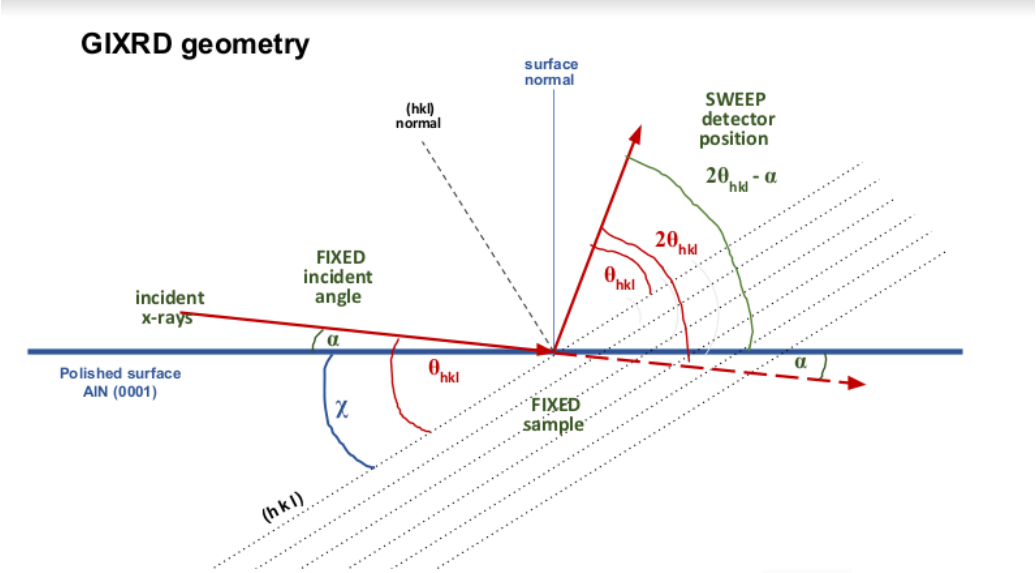

Figure 12. GI-XRD geometry showing definitions of χ, 2θ, and α.

X-ray diffraction peaks can also be used to calculate the approximate average grain size of a crystal. Thin films grow as individual grains, with grain boundaries between them. During epitaxial growth, grains can grow with certain orientations (a certain plane always parallel to the surface) like pillars on the substrate. Polycrystalline materials have differently oriented grains growing in all directions. The equation used to determine the approximate grain size is called the Scherrer equation where Grain Size$=$ $\frac{K\lambda}{FWHMcos(\theta)}$ where theta is half the angle of reflection as shown in Figures 10-12, λ is the x-ray wavelength 1.54Å, FWHM is the full width of the measured peak at half its intensity, and K is a shape factor which depends on the shape of the crystal. A typical value for K is 0.9 which was used in this work. The intent of grain size calculations was to compare grain sizes before and after heating, so finding an exact K value for the samples was not necessary. This calculation was performed to give the average grain size of the entire crystal and used for comparison of grain size before and after annealing.

3.4 Post-Deposition Annealing Treatments of Pt_xSi_{1-x} Thin Films

Three forms of heat treatments were performed in this research project: "N_2 heating", "vacuum heating", and "air heating". N_2 heating was the most common heat treatment. It involved heating a sample in the tube furnace shown in Figure 13 while the furnace was purged with high purity N_2 gas. The furnace was pressurized above atmospheric pressure to prevent oxygen from leaking in. The nitrogen was flowing at approximately two liters per minute through the furnace. Previous work has shown that at the center of the furnace the temperature is very uniform, so samples were heated in that uniform region. The samples were placed in an alumina crucible as shown in Figure 14 with another alumina crucible on top to protect the surfaces from any impurity particles in the furnace. The same furnace was used for heating in air with the only difference being that instead of flowing N_2 through the furnace, the sample was simply heated under normal air atmospheric conditions within the furnace tube.

Figure 13. Tube furnace for sample annealing within an N_2 environment pressurized to 0.08 MPa above atmospheric pressure.

Figure 14. PtSi / LGS samples (dark squares) in high purity alumina crucible ready for heat treatment.

Vacuum heating was performed in an ultra-high vacuum chamber with a base pressure of $< 5*10^{-9}$ torr. During heat treatments, the vacuum chamber reached a pressure as high as 10^{-6} Torr at high temperatures (above 700°C). The samples that were heated in vacuum were loaded onto tantalum holders and held down by tantalum wires. The tantalum holder was then radiatively heated to the desired temperature.

It is important to note that all samples were exposed to the atmosphere before all the heat treatments, including the vacuum heating, meaning that all samples had a thin native oxide layer which was present for each heat treatment.

3.5 Calibration of Pt and Si Film Deposition Rates

Because silicon, like water, expands when it is frozen, it can crack a crucible when freezing after a deposition. For this reason, silicon must be sublimed rather than melted. A vapor pressure curve versus temperature is well known for all elements in the periodic table and describes phase change between solid/liquids and gas. If the vapor pressure is set equal to $\sim 1*10^{-6}$ Torr, a film growth rate of approximately one monolayer of film growth per second is achieved at 1000°C [10]. Because a single monolayer deposition rate occurs for Si at ~1000°C, and Si melts at 1410°C, the Si will sublime (go

directly from solid to gas) under these conditions. The deposition rate for silicon was kept to be <0.3Å/s in this study which has been used successfully in the past [16].

The silicon and platinum rates had to be re-calibrated to make sure the correct film thicknesses were deposited. To do this, 200nm of pure Pt and, separately, 100nm of pure Si were deposited onto a substrate with one side covered. This effectively provided a ~200nm or 100nm cliff, whose height was then measured with surface profilometry. The silicon was measured to be 130nm during the calibration run. To fix this discrepancy, the sensitivity factor (a constant specific to our system that can be changed) was multiplied by $\frac{130}{100}$ to increase the deposition rate to the correct value. The 200nm growth of platinum was measured to be 205nm thick which is within an error of a 2.5%. To check the rates, a 170nm film was deposited which included 160nm of PtSi and 10nm of Zr. This growth was measured to be 168nm showing that the rates are correct within 3% error.

To get accurate film composition values, the XPS sensitivity factors for platinum and silicon had to be directly measured for the XPS detector. This was done by growing, separately, 50nm of pure Pt and 50nm of pure Si. These films were then (still under vacuum) transported to the XPS chamber for composition analysis. The sensitivity factor for Pt compared to Si is defined as $SF = \frac{I_{Pt}}{I_{Si}}$ where I is the peak intensity (Pt 4f and Si 2s peaks). The sensitivity factor SF was calculated to be approximately 15. This sensitivity factor was used to determine the ratio of platinum to silicon in a film. The Pt peak intensity is simply divided by 15, then directly compared to the Si peak intensity. For example, a Pt_2Si film should have intensities consistent with the equation $\frac{I_{Pt}}{15} = 2 * I_{Si}$.

4. RESULTS AND DISCUSSION

4.1 Investigation of $Pt_{25}Si_7$ Films

The multilayered adhesive used to attach langasite crystals (with SAWR sensors built on top) to steel needs to be annealed to "set" the glue by letting the layers react with each other. During this annealing process, the changing temperature can damage the adhesive due to CTE differences, so it is advantageous to anneal at as low of a temperature as possible. To lower the temperature necessary to set the glue, $Pt_{25}Si_7$ was chosen because according to the phase diagram its melting point is lower than the rest of the platinum-silicon system as shown in Figure 15 [26]. $Pt_{25}Si_7$ is a mix of pure platinum and Pt_3Si with a concentration of approximately 22% silicon and 78% platinum. The $Pt_{25}Si_7$ eutectic has not been explored extensively so its high temperature stability is not well known. A potential pitfall to consider for this eutectic is that there can be platinum agglomeration and non-uniformity across a film. The pure platinum in $Pt_{25}Si_7$ tends to

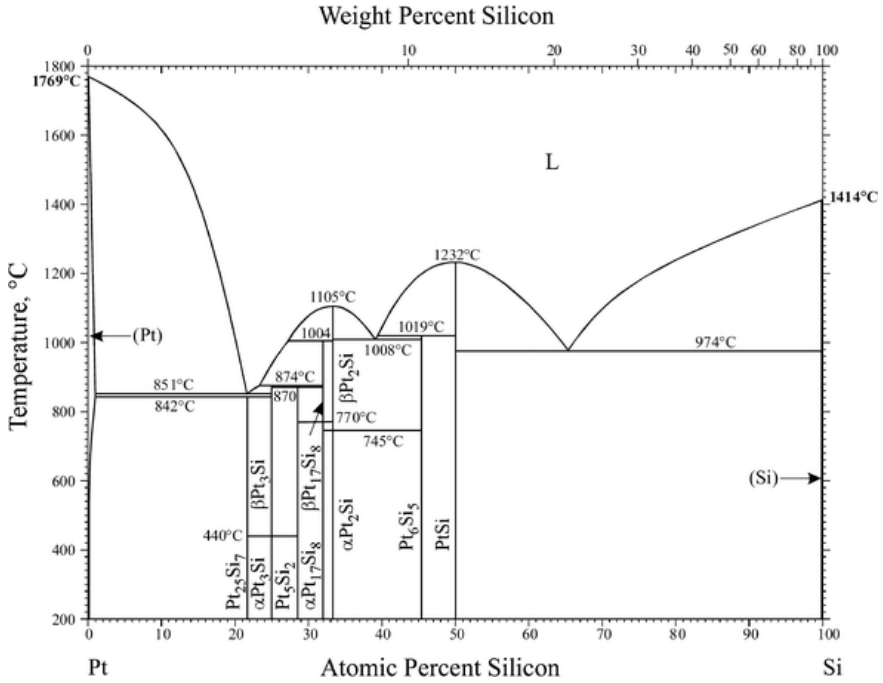

Figure 15. Platinum-Silicon bulk equilibrium phase diagram [26].

have a high driving force for agglomeration at high temperatures, disrupting the glue stability. Because $Pt_{25}Si_7$ is a mixture of the Pt_3Si phase and a pure Pt phase, the film is by definition non-uniform. This non-uniformity, while it can cause variation in each adhesive produced, could assist with the attachment to the next layer. The platinum-silicon layer is meant to attach langasite to a copper layer [8] and pure platinum may more readily react with copper than the Pt_3Si, attaching the layers together. Adding a copper overlayer could also reduce platinum agglomeration because the platinum would instead react with copper.

To assess the stability of $Pt_{25}Si_7$ grown on langasite at high temperatures, samples were prepared using Electron Beam Physical Vapor Deposition (EBPVD) depositing platinum and silicon in the ratio 25:7 at room temperature. To reduce as many outside variables as possible, the $Pt_{25}Si_7$ sample was then heated in vacuum so that no reactions with oxygen or other elements in the atmosphere could disrupt the experiment. The melting point of $Pt_{25}Si_7$ is approximately 851°C (see Figure 15). The sample was placed on a tantalum holder for the heating procedure which was heated to 910°C at a rate of 20°C/minute. The temperature 910°C was chosen to make sure the entire sample melted completely so that it could then form the $Pt_{25}Si_7$ eutectic.

After heating, the langasite crystal appeared to have reacted with the tantalum holder and cracked. An XPS scan showed that the surface of the tantalum had a composition of $Ga_4Ta_{11}O_{61}C_{23}$. The presence of gallium and the high level of oxygen clearly shows evidence of a reaction with langasite. X-ray diffraction after heating on the largest shard of langasite showed a variety of unknown peaks. Pure silicon was the only identifiable crystal structure, while some PtSi, Pt_2Si, and langasite peaks were possibly

present with large errors. Due to the interaction with the tantalum holder and the langasite cracking, it was clear that a stable $Pt_{25}Si_7$ eutectic did not form.

A second $Pt_{25}Si_7$ sample was heated to 900°C in an alumina crucible within a nitrogen-purged tube furnace. Nitrogen is very non-reactive, so it was expected that the $Pt_{25}Si_7$ sample would not change within the nitrogen atmosphere. The heating rate was changed from 20°C/min to 10°C/min due to the langasite cracking in the first experiment. While it is unclear what caused the langasite to crack, one explanation is that the differences in Coefficient of Thermal Expansion (CTE) between the langasite and the $Pt_{25}Si_7$ layer or the tantalum caused the cracking when cooled. When heated more slowly, the layers have enough time to stretch and come to equilibrium. The sample also can reach a more uniform temperature throughout to reduce stresses caused by non-uniform cooling which produces non-uniform contraction.

After heating in nitrogen, the sample had clear evidence of platinum agglomeration as shown in Figure 16. This is not an unexpected result due to the large amount of platinum, but it does mean that without another layer, $Pt_{25}Si_7$ films are not thermally stable on langasite.

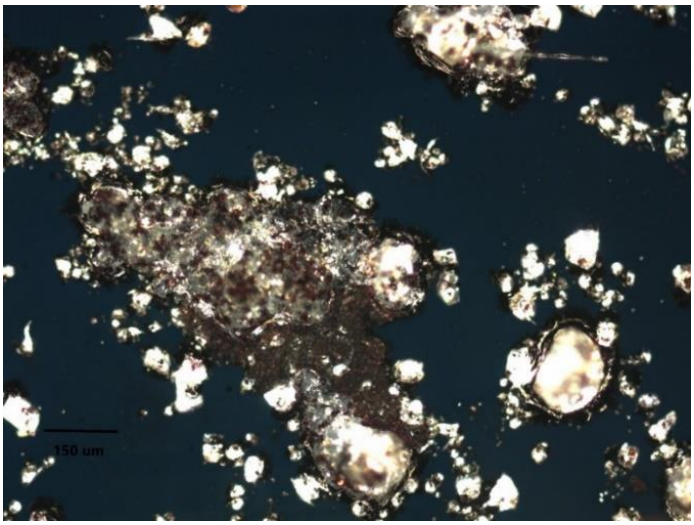

Figure 16. Pt agglomeration on $Pt_{25}Si_7$ sample heated to 900°C in N_2.

XRD analysis after heating showed cubic platinum peaks as well as peaks from Pt_3Si as shown below in Figure 17. The Pt_3Si peaks, however, were very faint, and pure silicon was still present. This experiment shows that the platinum and silicon layer did not fully melt and form the expected eutectic consisting of only pure Pt and Pt_3Si phases.

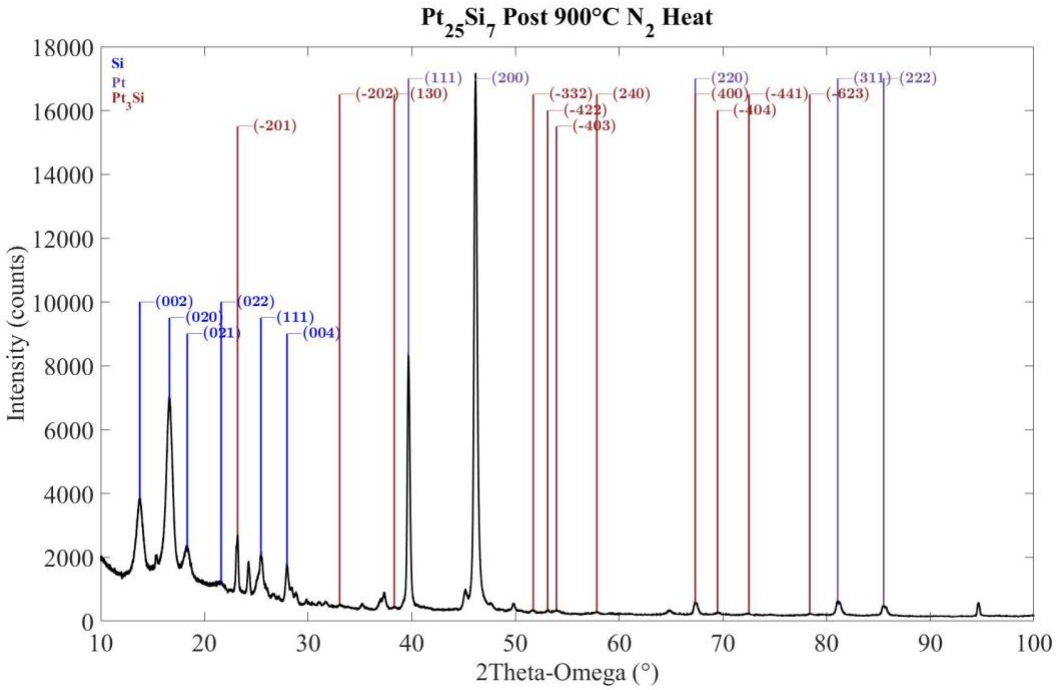

Figure 17. XRD Scan of $Pt_{25}Si_7$ after 900°C N_2 heat showing Si (0.1° error), Pt (0.1° error), and Pt_3Si (0.14° error) phases as identified from reference spectra in PDF (01-090-3126), (00-004-0802), (04-015-7964) [33].

The primary crystal structure appears instead to be just pure platinum and pure silicon. Further experimentation at higher temperatures or with longer dwell times should be carried out in the future to ensure time for the eutectic to fully melt. This experimentation, however, would lead to further platinum agglomeration, so the $Pt_{25}Si_7$ composition was set aside until testing could be done with a copper layer which should reduce platinum agglomeration.

The sample had significant grain size changes before and after heating. The silicon grain sizes calculated using the width of the XRD peaks were consistently

approximately 12.4nm before and after heating, while the platinum grains increased from about 43.5nm to 79.5nm. This significant increase in platinum grain size is expected during platinum agglomeration, providing further evidence of such agglomeration [20].

4.2 Investigation of PtSi Films

Of the part of the platinum-silicon phase diagram that has been explored in the past, PtSi has been identified as the most stable alloy at high temperatures when compared to Pt_2Si and Pt_3Si [16], [17]. The thermal stability of PtSi grown on langasite with varying deposition temperatures and annealing conditions was explored to find the best set of conditions for growing a uniform PtSi crystal structure that is stable when thermally cycled. It is important to note that an old silicon source was used for PtSi growths before 02_10_2023 which had an unstable deposition rate and resulted in films being about 5% oxygen at the surface and 95% PtSi measured using XPS. A new silicon source after that date yielded films with much lower oxygen levels.

4.2.1 PtSi Films from 01_05 Deposited at 320°C

In previous work performed in the same vacuum deposition chamber, PtSi films were deposited and studied resulting in the finding that PtSi films grown at 400°C on r-sapphire were morphologically stable up to 1000°C in air and showed no signs of platinum agglomeration [16], [17]. To evaluate this result when growing PtSi films on langasite, platinum and silicon in a 1:1 ratio was deposited, but due to a difference between the temperature shown on the controller and the actual sample temperature, PtSi films were grown at 320°C instead of 400°C. XPS showed approximately 50% Si and 50% Si, confirming that the film was indeed PtSi.

The XRD results show evidence of PtSi as well as a Pt_2Si phase and pure Si. The spectrum, however, was quite different than previous PtSi XRD spectra from the past work, as shown in Figure 18. The (101), (211), and (002) peaks are the only shared peaks, and the relative intensities are vastly different.

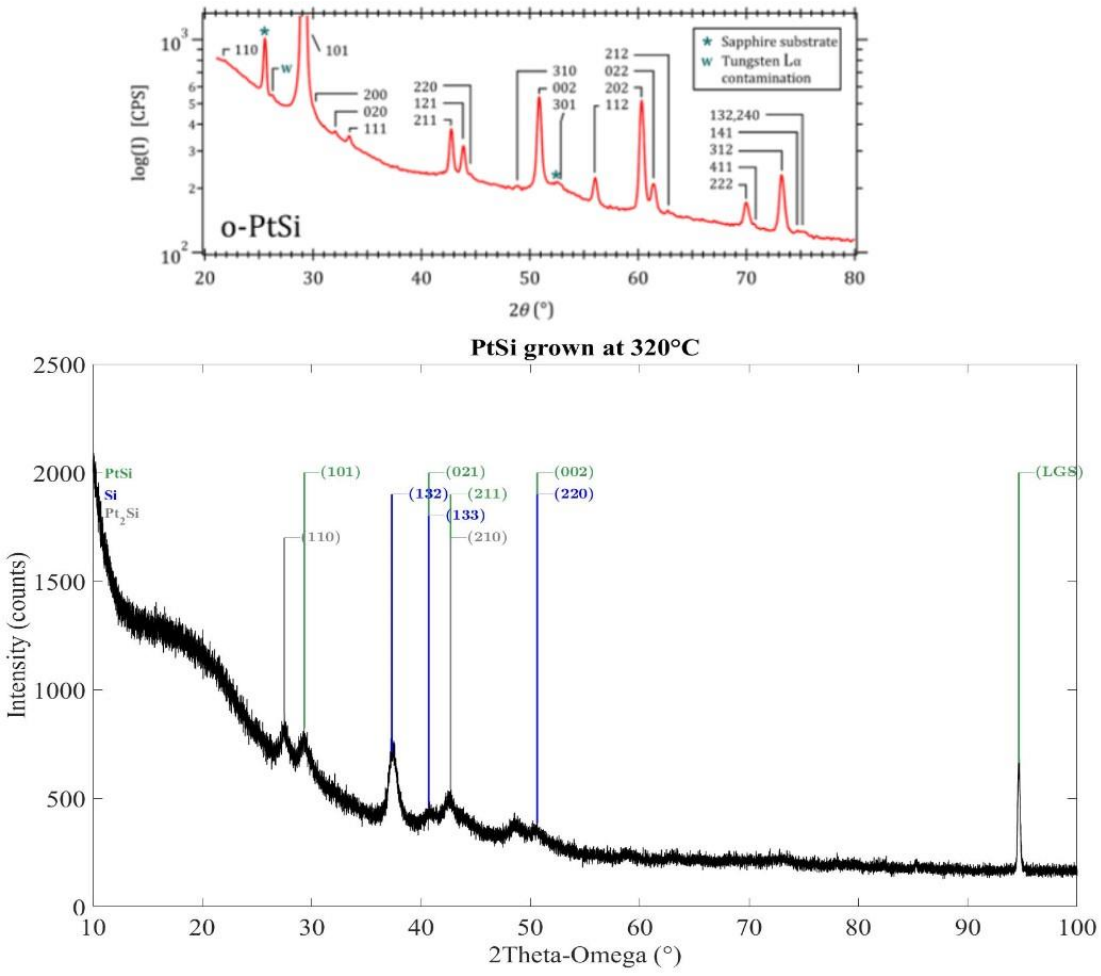

Figure 18. Comparison of previous PtSi growth at 400°C [17] and PtSi growth at 320°C showing significant differences. The 320ºC sample has PtSi (0.2° error), Si (0.06° error), and Pt_2Si (0.17° error) phases present as identified from reference spectra in PDF (04-003-0990), (01-090-3126), (01-087-4671) [33].

To see if the PtSi film might more closely resemble past work after heat treatment, the PtSi film was heated in vacuum at 10°C/min to 800°C where it was held for 30 minutes, then cooled to room temperature at 10°C/min. The temperature of 800°C

was chosen because the $Pt_{25}Si_7$ film on LGS cracked at 910°C and thus a lower temperature was attempted. PtSi melts at 1200°C so if the sample is heated past approximately half the melting point (600°C) there should be enough atomic diffusion occurring for the platinum and silicon to react. The 800°C temperature is far enough past 600°C that if the sample temperature is lower than the furnace set point either in the vacuum chamber or in the nitrogen furnace, the sample should still be at least 600°C and have enough energy to react.

After the heating, XRD showed evidence of PtSi, Pt_2Si, and a few unidentifiable peaks. PtSi crystallization is clearly shown, however, the addition of Pt_2Si is unexpected and the spectrum still does not match well with the XRD spectrum found in previous work. While prior PtSi films had strong (101), (121), (002), and (112) peaks after heating, the PtSi heated to 800°C had only small (101) and (121) peaks, no (002) or (112) peaks, and evidence of nine other PtSi peaks as well as evidence of a Pt_2Si phase. This discrepancy was thought to be potentially caused by oxygen contamination in the silicon or non-uniform sublimation from the source which will cause a varying deposition rate. The langasite also cracked which appears to have destroyed the PtSi layer as shown in the bottom right corner of Figure 19, so the experiment was not very controlled. The PtSi layer should be very reflective and smooth, but instead the langasite surface is rough and grey with no visible evidence of a PtSi layer.

After removing the sample from vacuum, the langasite was cracked and there was LGS residue on the tantalum holder as shown in Figure 19. Part of the langasite was tightly stuck to the tantalum holder, clearly showing that a reaction took place. The lower temperature and slower cooling rate than previous vacuum heats did not stop this

interaction between langasite and tantalum. Langasite appears to have fused to the tantalum, and then pulled apart when cooled due to a difference in CTE values between the tantalum and the LGS, just like how typical adhesives crack when sticking LGS to steel. Tantalum's CTE, however, is about $6.3\frac{\mu m}{m°C}$ [27] which is close to the CTE of

Figure 19. LGS reaction with tantalum holder when heated to 800°C in vacuum showing cracks in the LGS sample.

langasite, 4-$5.6\frac{\mu m}{m°C}$. This is a small enough difference that it should not be the cause of langasite fracturing. XPS done on the holder showed a $O_{57}C_{25}Ta_{13}Ga_5$ composition which is approximately the same as in the previous vacuum heating experiment. In this image, however, there is more visual evidence of part of the langasite reacting with and sticking to the tantalum holder. This is an interesting phenomenon but was beyond the scope of this project, so heat treatments in vacuum were halted, and depositions were kept to 400°C and below.

4.2.2 PtSi Films from 01_10 Deposited at 320°C

To resolve the differences between the grown PtSi films and prior work in the same chamber, PtSi was deposited in a 1:1 ratio both on langasite and r-sapphire in the same deposition run. The different substrates could lead to different preferred orientations

of the PtSi crystal which would change which peaks are visible in a standard 2θ scan. Again, the samples were grown with the substrate temperature set to 400°C but the sample temperature was actually 320°C. XPS showed about 47.4-49.4% Si indicating that the sample was very close to a 1:1 Pt:Si ratio.

The XRD spectra from the PtSi films grown on langasite and sapphire were nearly identical as shown in Figure 20. However, they departed significantly from the growth on 01_05_2023 as shown in Figure 21 in that they had significantly more PtSi and Pt_2Si peaks with higher intensities. This result suggested that the difference was not caused by growth on langasite instead of r-sapphire, but rather that other parameters were not adequately controlled so that every deposition has varying results.

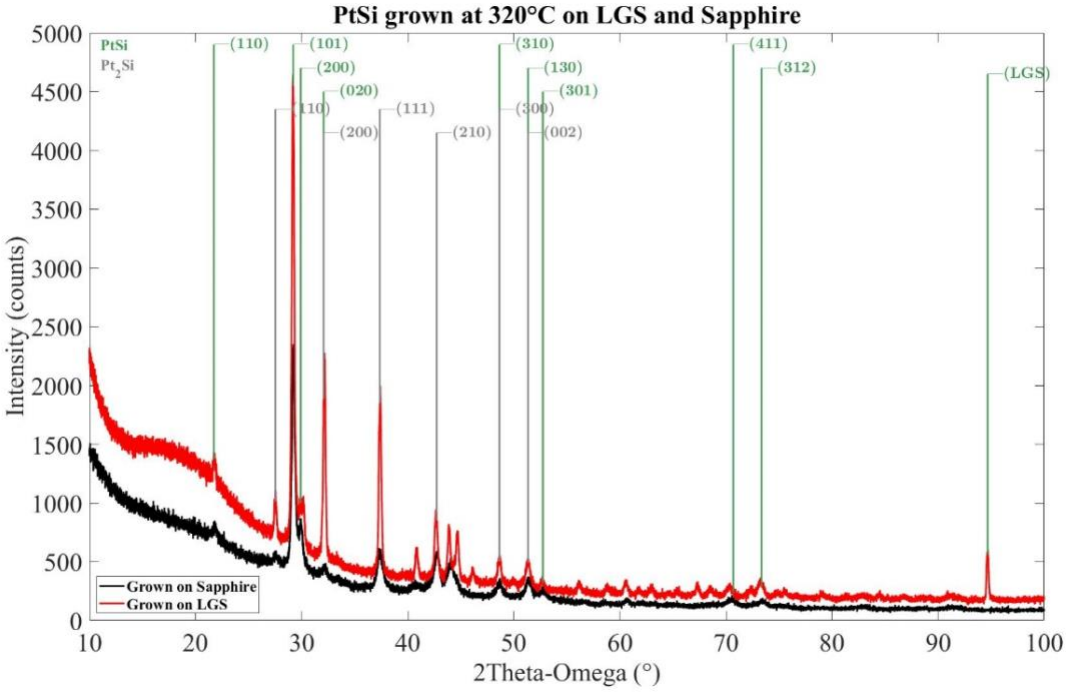

Figure 20. XRD spectra from PtSi co-deposited at 320°C on LGS and r-sapphire substrates showing PtSi and Pt_2Si crystal structures as identified from PDF (04-003-0990), (01-087-4671) [33].

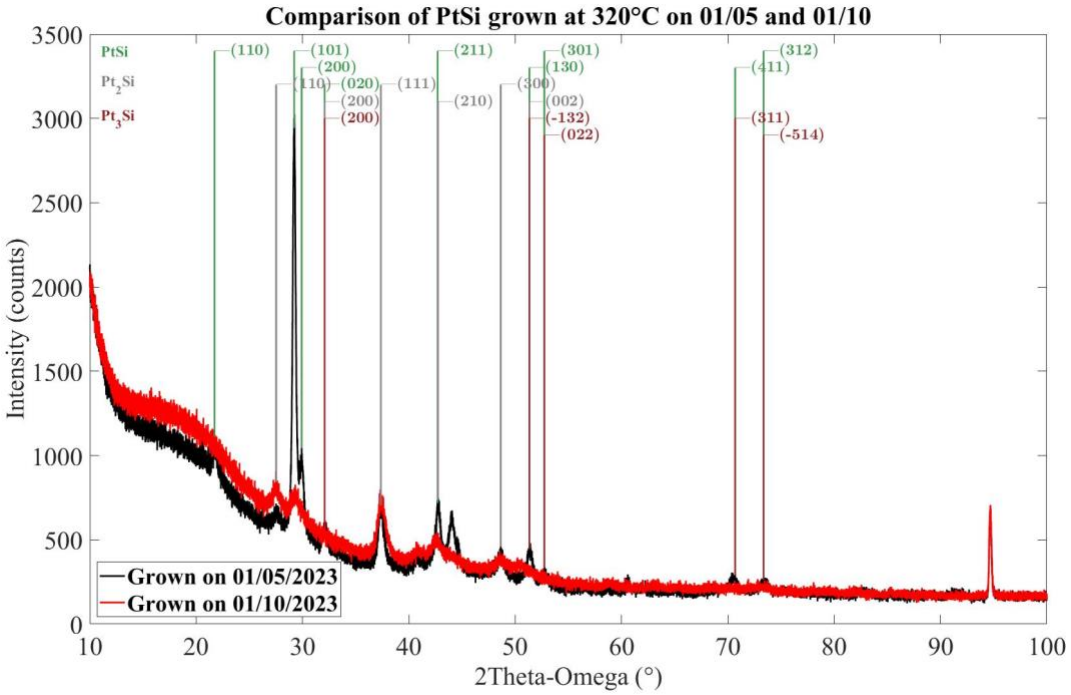

Figure 21. XRD spectra comparing PtSi grown on 01_05 at 320°C to PtSi grown on 01_10 at 320°C showing PtSi, Pt_2Si, and Pt_3Si phases as identified from PDF (04-003-0990), (01-087-4671), (04-015-7964) [33]. The growth on 01_10 has fewer, less intense, and broader peaks and lacks the Pt_3Si phase. Phases identified from PDF (04-003-0990), (01-087-4671), (04-015-7964) [33].

These experiments clearly show formation of different crystal structures in depositions with the same conditions. The advantage of using EBPVD to grow samples is its ability to create uniform, repeatable samples, so this result was disturbing. With limited time, however, new experiments were done to search for the most thermally stable deposition temperature and annealing conditions. When the conditions that create more uniform, stable samples are identified, the variation in experiments should be reduced because the samples will form a uniform PtSi crystal structure each time.

To see if annealing the samples could resolve the differences between both PtSi films, the 01_10 PtSi film was heated to 800°C in the N_2 furnace. The XRD spectra in Figure 22 show that the films grown the same way, both heated to 800°C, though with different heating procedures, still have extremely different crystal structures.

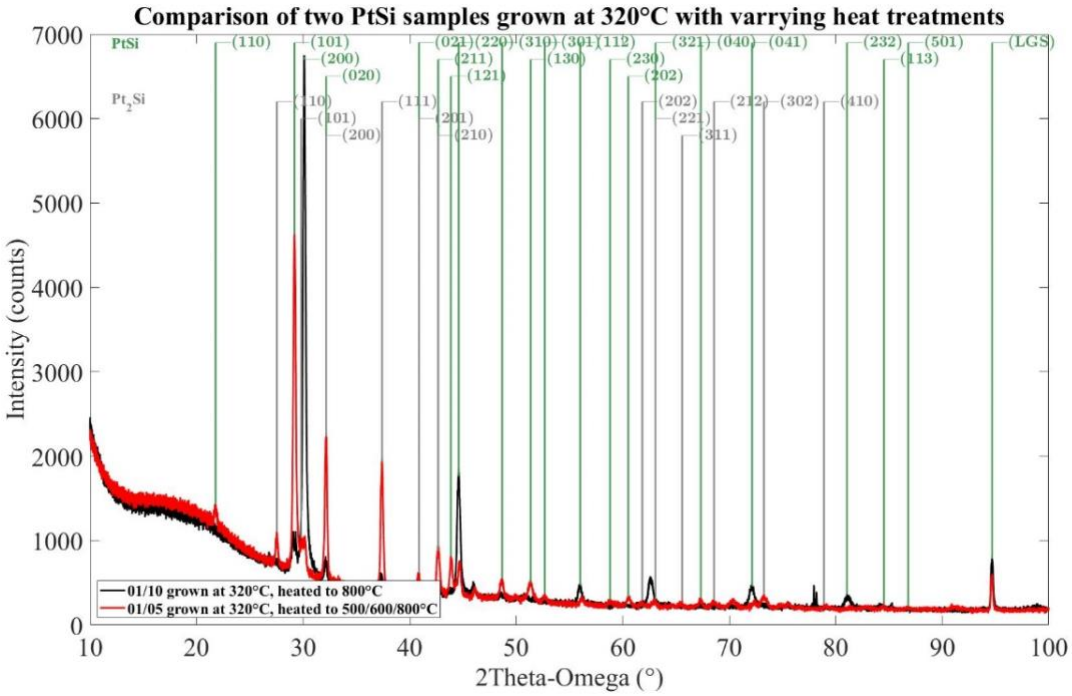

Figure 22. XRD spectra comparing PtSi grown on 01_10 at 320°C after 800°C N_2 heating to PtSi grown on 01_05 at 320°C after 500/600/800°C N_2 heating. The slower heating rate yielded fewer peaks, and only PtSi, while the sample heated straight to 800°C shows many PtSi and Pt_2Si peaks. Phases identified using PDF (04-003-0990), (01-087-4671) [33].

While having a vastly different crystal structure than previous samples, the PtSi sample heated to 800°C in the N_2 furnace came out visually unchanged. This was the first experiment where the sample had no visible platinum agglomeration or a cracked langasite substrate. After heating to 850°C in N_2 and 400°C in air to test the stability, the film still had the same crystal structure, with a slight increase in peak intensities. The lack of change indicated that PtSi grown at 320°C and heated at a rate of 10°C/min to 800°C and 850°C has a stable crystal structure for at least a few rounds of thermal cycling. Figure 23 compares LGS after the first heat to after the third heat to 400°C in air. The only difference is a slight increase in peak intensity indicating that the first heat treatment did not fully react the entire sample. The grain size was approximately 28nm as deposited and 27nm after heating to 800°C and 850°C in N_2 and 400°C in air, showing that the PtSi

grains were stable and were not growing after each heat which could lead to platinum agglomeration.

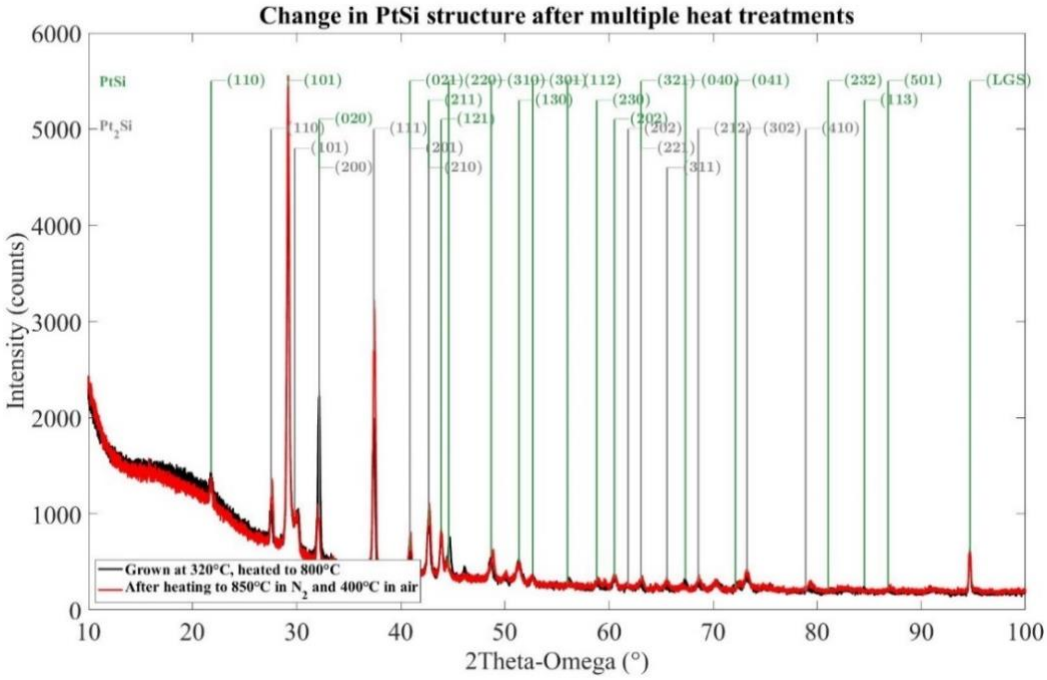

Figure 23. XRD spectra comparing PtSi sample grown at 320°C after heating to 800°C in N_2 and PtSi sample after heating to 850°C in N_2 then 400°C in air. PtSi and Pt_2Si phases are present as identified using PDF (04-003-0990), (01-087-4671) [33].

The thermal stability of the PtSi sample was an important result, however, the presence of a small amount of Pt_2Si phase was concerning because it introduces non-uniformity into the sample which increases variation and can decrease adhesion strength due to non-uniform bonding to the next layer. This non-uniform bonding can also increase susceptibility to cracking when thermally cycled.

4.2.3 PtSi Films from 01_25 Deposited in Layers at Room Temperature

Solid state diffusion is a popular way of making platinum-silicon thin films due to the structure being relatively independent of the deposition method [28]. Co-deposited platinum-silicon films, however, have been identified as having higher thermal stability than solid state reacted films [20]. Growing PtSi in layers is a technique that sits in-

between each method. To test if growing PtSi in layers could have the advantages of both solid state reacted films and co-deposited films, PtSi in a 1:1 ratio was grown at room temperature both co-deposited and in five nanometer layered stacks.

The layered PtSi was grown in 5nm layers, so the total stack consisted of LGS/10nmZr/5nmPt/5nmSi . . . ending with a top layer of 5nm Si for a total of 50nm of Pt and 50nm of Si. After depositing layered and co-deposited PtSi (each with a 10nm Zr adhesion layer), the XRD spectra were compared and as expected, the layered PtSi did not form a crystal structure because there was not enough atomic diffusion with the room temperature growth. Surprisingly, the XRD spectrum of PtSi co-deposited at room temperature had significant PtSi and Pt_2Si peaks as shown in Figure 24. Even at room temperature, while co-depositing, PtSi and Pt_2Si crystal structures can form.

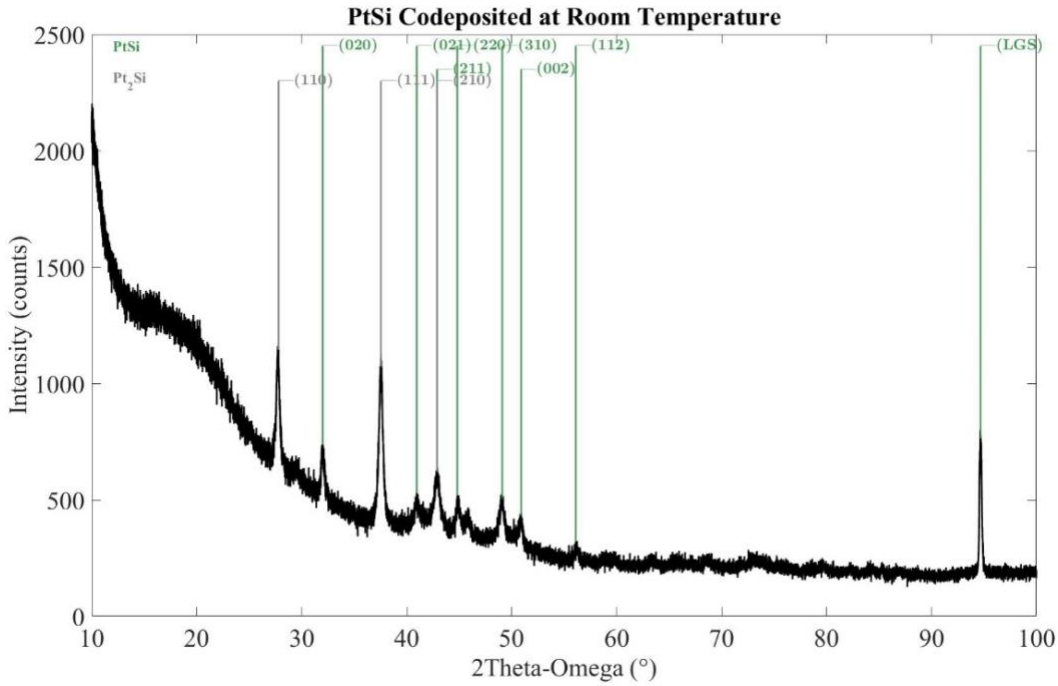

Figure 24. XRD spectrum from PtSi co-deposited at room temperature shows PtSi (0.1° error) and Pt_2Si (0.06° error) phases present as identified from PDF (04-003-0990), (01-087-4671) [33].

The layered and co-deposited PtSi samples were heated at 10°C/min to 500°C for 10 minutes and 600°C for 10 minutes following the temperatures used in a previous study using solid state reaction of platinum-silicon films [28]. At 500°C, each platinum layer can diffuse through 5nm of silicon to react fully in less than a minute. The films were then immediately heated from 600°C to 800°C at a rate of 10°C/min so that they could be compared to earlier samples. The idea was that the 500°C/600°C treatment would form PtSi, as reported previously, then the heat to 800°C would allow for comparison to previous samples. The co-deposited sample, and a sample grown at 320°C were also included in the heat treatment for comparison.

Surprisingly, the layered PtSi sample had only pure platinum peaks in the XRD pattern with no evidence of PtSi, Pt_2Si, or pure Si after heating. It also had clear signs of platinum agglomeration when observed with an SEM as shown in Figure 25. SEM of the co-deposited films at room temperature and 320°C showed no evidence of platinum agglomeration. From this experiment it was determined that growing PtSi in layers was

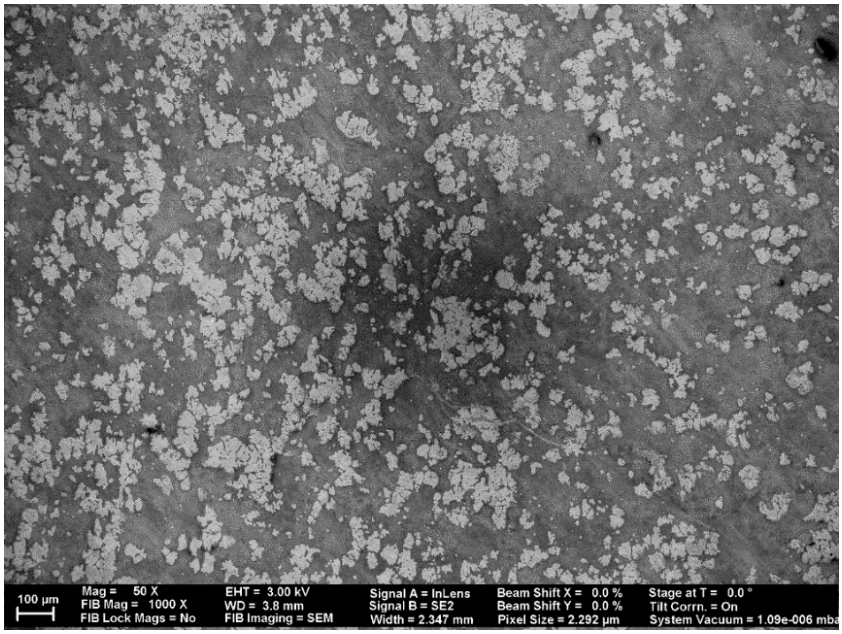

Figure 25. SEM of PtSi layered film after heating to 500/600/800°C showing clear signs of platinum agglomeration.

worse than co-depositing, and not worth exploring further in this work. Because of platinum agglomeration, even higher temperatures would be needed to form the PtSi crystal structure, thus increasing the risk of CTE-induced cracking.

The 320°C co-deposited PtSi sample grown on 01_05, heated with the same 500/600/800°C treatment for comparison had an interesting XRD spectrum shown in Figure 26. It had a strong PtSi 200 peak which had not been seen before, had no evidence of a Pt_2Si phase, and had fewer PtSi peaks than previous samples. The co-deposited sample grown at room temperature, however, had Pt_2Si and many PtSi peaks as shown in Figure 27. These results indicate that growing at higher temperatures and then annealing for just twenty minutes below 600°C helps get rid of Pt_2Si formation and create oriented crystals. As shown in Figure 26, there are only 11 PtSi peaks present, indicating that the crystal grains are growing along a few preferred orientations. Instead of being polycrystalline, like the other samples, with many PtSi peaks present, the sample is more uniformly oriented which is preferred for the PtSi layer.

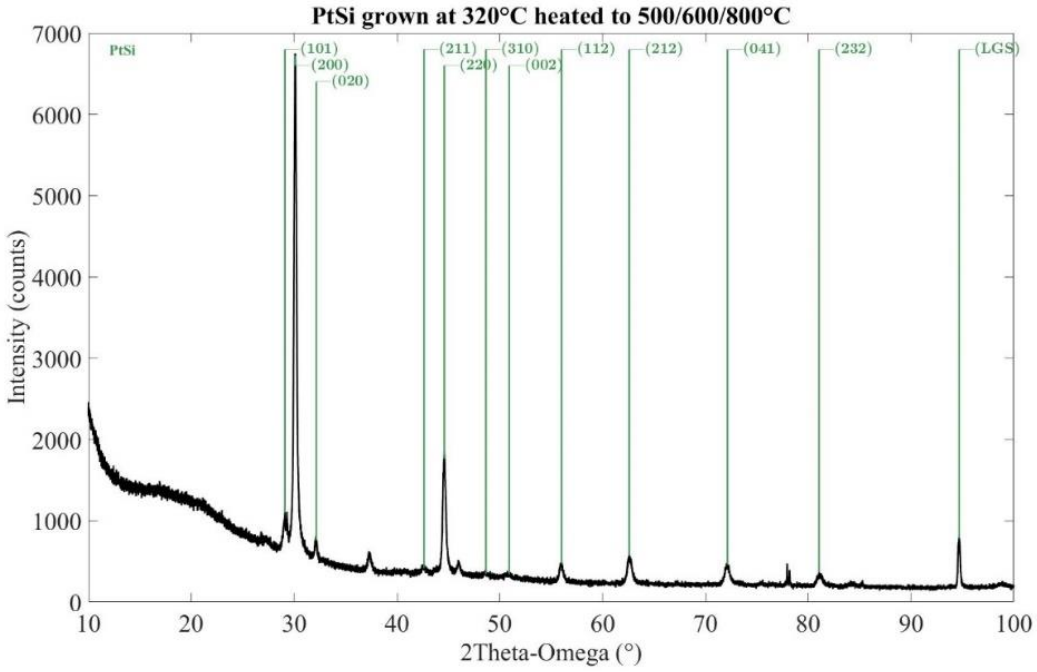

Figure 26. XRD spectrum from PtSi grown 01_05 at 320°C after heating to 500/600/800°C in N_2 shows few peaks from a PtSi phase with a strong 200 peak as identified from PDF (04-003-0990) [33].

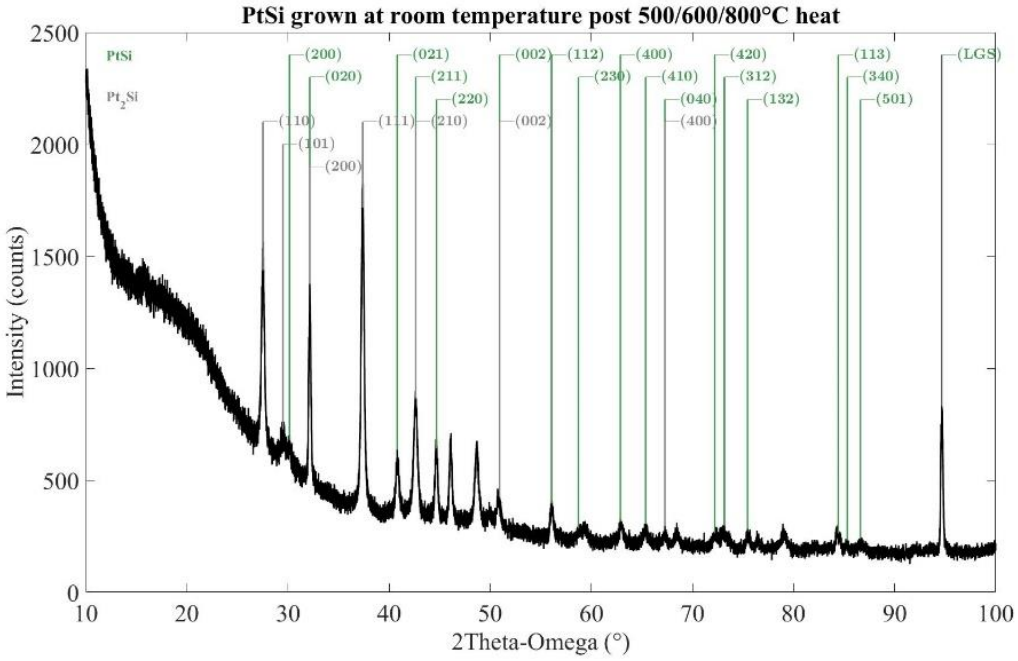

Figure 27. XRD spectrum from PtSi grown at room temperature after heating to 500/600/800°C in N_2 with many peaks from a PtSi (0.1° error) phase and Pt_2Si (0.18° error) phase as identified from PDF (04-003-0990), (01-087-4671) [33].

4.2.4 Influence of Deposition Temperature and Heat Treatments

The PtSi sample co-deposited at 320°C (grown on 01_05) was heated to at 10°C/min to 500°C for 10 minutes and 600°C for 10 minutes, then to 800°C for 30 minutes. A sample grown on 01_24 at room temperature was also present during the heat treatment. The XRD spectra from both samples are shown in Figure 28. The sample grown at 320°C formed more intense PtSi peaks and less Pt_2Si peaks (none) compared to the one grown at room temperature. This indicates that growing at a higher temperature is

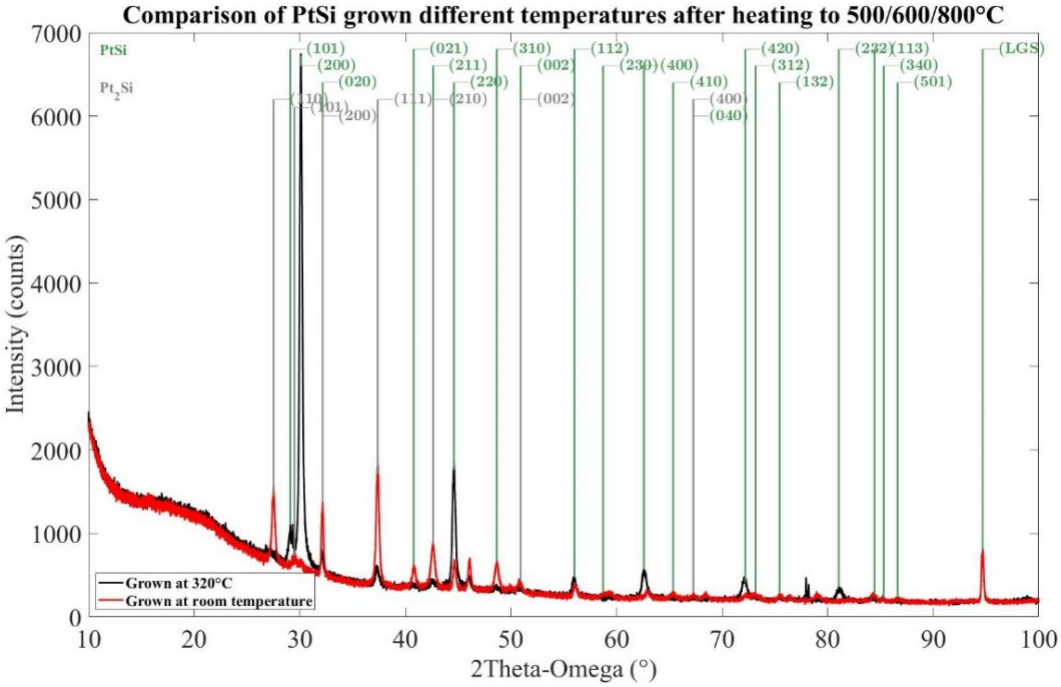

Figure 28. XRD spectra comparing PtSi grown at 320°C and PtSi grown at room temperature both after heating to 500/600/800°C in N_2. The sample grown at room temperature has more PtSi peaks, and a Pt_2Si phase present, while the sample grown at 320°C has few PtSi peaks with a strong 200 peak. Phases identified from PDF (04-003-0990), (01-087-4671) [33].

more conducive to forming a strong, well-oriented PtSi crystal structure and not forming the unwanted Pt_2Si phase.

The 500/600/800°C heat treatment also allows a comparison to be made between two films, both grown at 320°C, but one heated to 500/600/800°C and one heated directly to 800°C as shown in Figure 22 (page 33). The film that was heated more slowly formed

that well-oriented PtSi crystal structure while the film heated more quickly formed polycrystalline PtSi along with an unwanted Pt_2Si phase. From these two comparisons, it appears that when films linger between 300°C and 600°C, they are more likely to form single phase, oriented PtSi rather than polycrystalline PtSi and Pt_2Si phases.

The film grown at 320°C and heated to 500/600/800°C formed an oriented, single phase PtSi crystal structure that was successfully heated to 800°C. From comparisons made between that and previous experiments, it appears that lingering between 300°C and 600°C aids in the formation of that preferred structure. To see if increasing the deposition temperature could form the same structure, a film was grown at 400°C on 02_16. The higher temperature during the deposition would be expected to aid in the formation of an oriented PtSi structure which was successfully formed as seen in Figure 29.

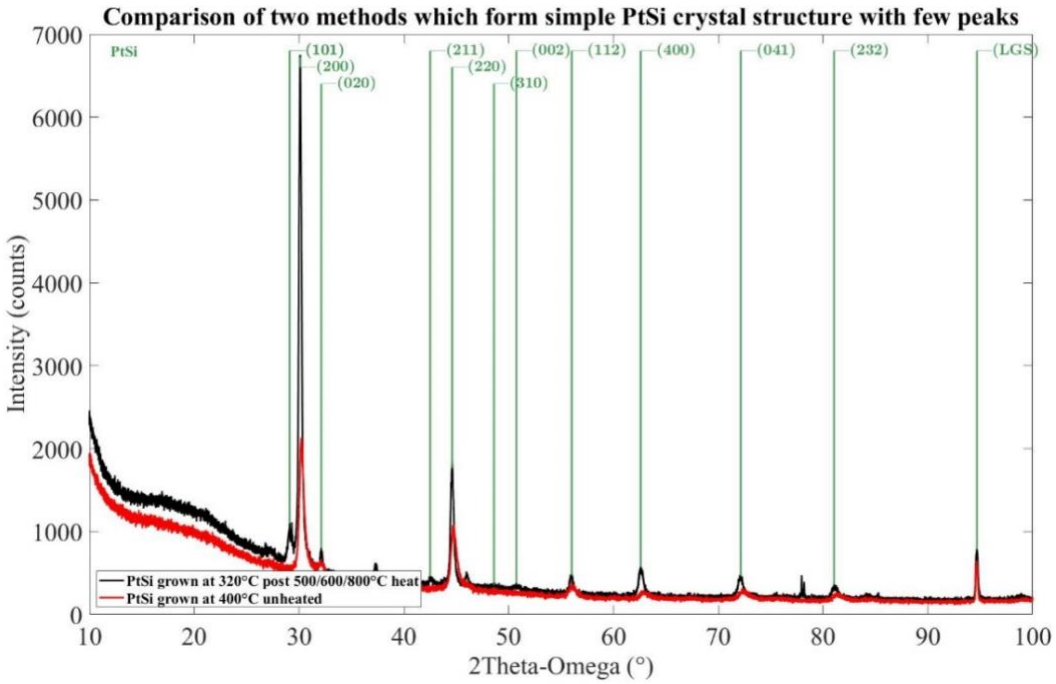

Figure 29. XRD spectra comparing PtSi grown at 400°C with no heating and PtSi grown at 320°C after heating to 500/600/800°C in N_2. The spectrum shows both samples have the same PtSi phase with few peaks as identified from PDF (04-003-0990) [33].

Tests of the thermal stability of the sample grown at 400°C were done by heating in the nitrogen-purged furnace. When heated to 800°C, the PtSi grown at 400°C completely changes its crystal structure. This happened when heated directly to 800°C after deposition and when heated to 800°C after previous heating to 600°C. In each case, the sample ends up with many more PtSi peaks as shown in Figure 30 indicating a polycrystalline film. The heating to 600°C, however, preserved the oriented structure with a slight increase in peak intensity being the only change. This result suggests that PtSi films grown at 400°C, while able to form an oriented single phase PtSi structure, are not as thermally stable as films grown at 320°C, or that lingering at 500°C is necessary for the stability of the oriented PtSi phase.

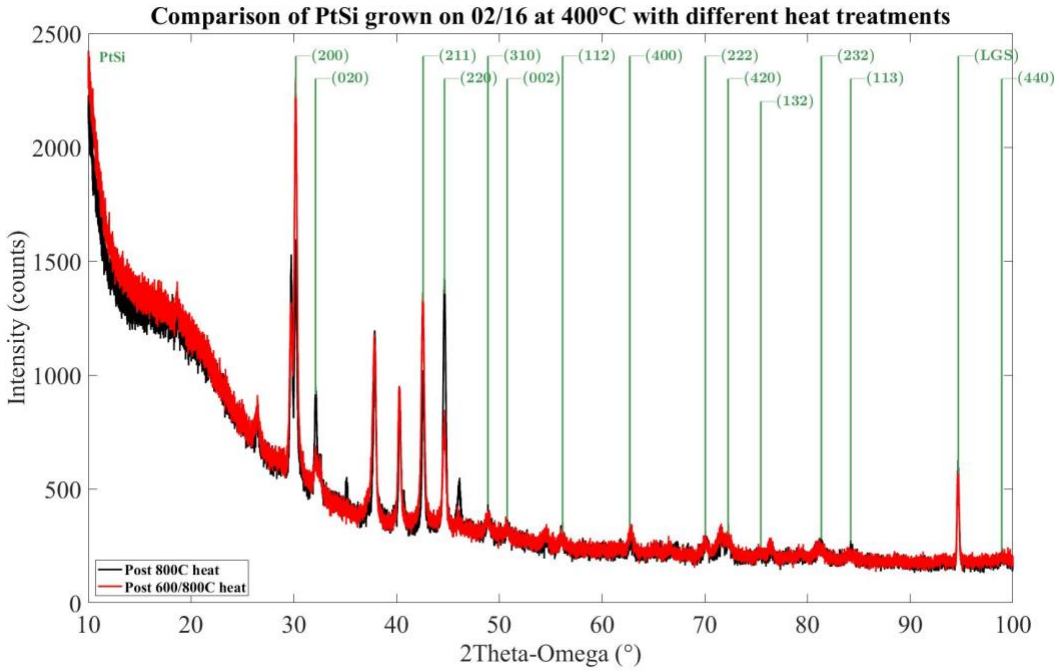

Figure 30. XRD spectra comparing PtSi grown on 02_16 after an 800°C heat to a sample grown at the same time after a 600/800°C heat. Both samples have the same many PtSi (0.1° error) peaks. Identified from PDF (04-003-0990) [33]

4.2.5 Comparison of PtSi Films Deposited at 320°C and 400°C

Both PtSi films grown at 320°C and grown at 400°C can form a single phase PtSi crystal structure with no Pt_2Si so they are the most promising samples. To directly compare the two, PtSi samples were deposited at 320°C and 400°C on the same day, one right after the other. These samples, while they still did not show any evidence of Pt_2Si peaks, had different crystal structure than in previous experiments. Both samples had the same structure before and after heating. The structure before heating is shown in Figure 31. The sample has sixteen PtSi peaks with similar intensities indicating a more polycrystalline sample.

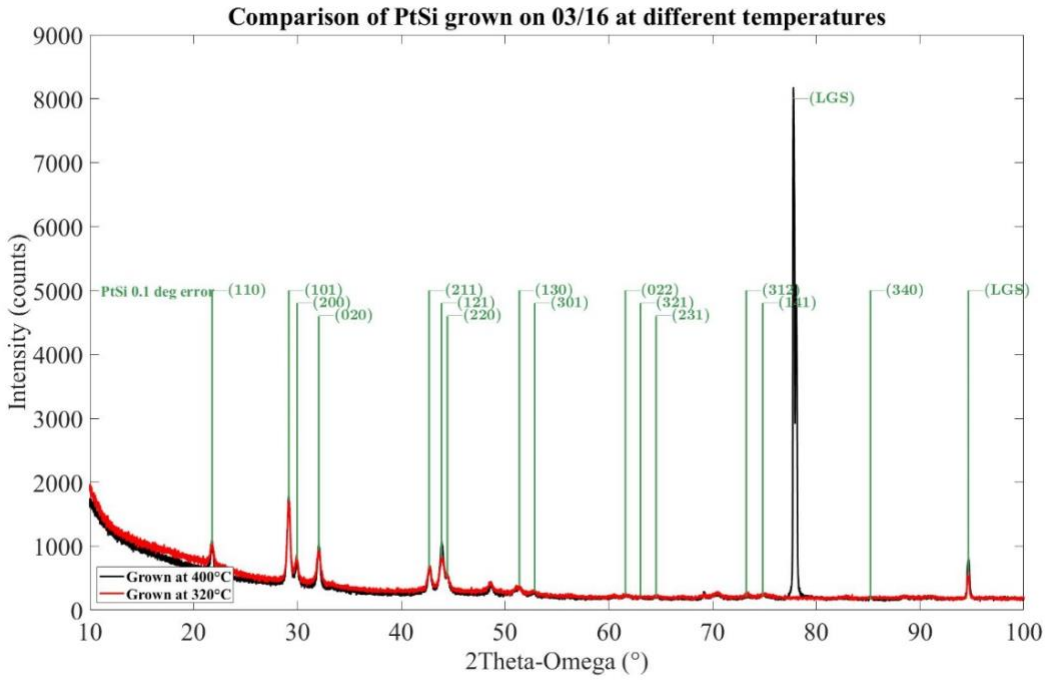

Figure 31. XRD spectra comparing PtSi grown on 03_16 at 320°C to PtSi grown at 400°C. The spectra show sixteen PtSi (0.1° error) peaks with similar intensities as identified from PDF (04-003-0990) [33].

Heating to 500°C for 10 minutes, 600°C for 10 minutes, then 800°C for 30 minutes simply increased the intensity of a few peaks but did not change the structure further. The grain size as measured by XRD was 31nm before heating and 30nm after

heating, indicating that there was no grain growth or platinum agglomeration. The variability in growths from different days is concerning. However, the experiment shows that PtSi grown at 320°C or 400°C and heated at 10°C/minute to 500°C for 10 minutes then 600°C for 10 minutes can withstand heating up to 800°C without changing its single phase PtSi crystal structure. One sample grown at 400°C (PtSi grown on 02_16), however, did lose its structure after heating to 800°C, so samples grown at 320°C show more promise for thermal stability at higher temperatures. An adhesive layer that can function up to at least 600°C is a vast improvement over previous adhesives.

4.2.6 Orientation of PtSi Films

The PtSi films with fewer peaks visible in the typical 2θ XRD scans are thought to be more oriented than other samples, and therefore more uniform. This orientation means that the sample would be growing with, for example, (200) planes always parallel to the surface, growing in predictable columns. To evaluate the orientation, grazing incidence XRD scans were done on the samples with few PtSi peaks. The grazing incidence scans showed the same peaks as the 2θ scans but with two more PtSi peaks present as shown in Figure 32. If the crystal was polycrystalline, with grains growing in every direction, the 2θ scan would have the same number of peaks as the grazing incidence scan and would have more than eleven PtSi peaks. This grazing incidence scan, however, shows that there are peaks present that are not parallel to the surface, indicating that only preferred planes are oriented parallel to the surface. This provides evidence that growing at 320°C or 400°C and lingering between 500°C and 600°C does create more oriented, single phase PtSi films.

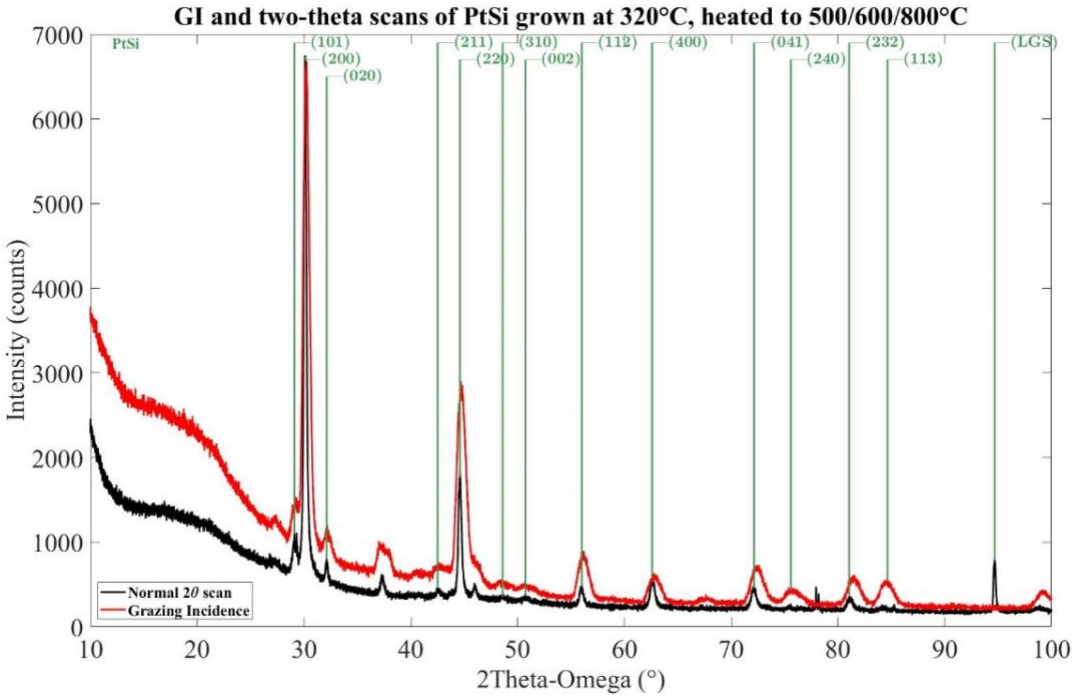

Figure 32. XRD spectra comparison of 2θ scan and grazing incidence scans from PtSi grown at 320°C after heating to 500/600/800°C in N_2. The spectra show few PtSi peaks, however, the grazing incidence scan has two more PtSi peaks than the 2θ scan. Phases identified from PDF (04-003-0990) [33].

To further explore the crystallographic orientation of the sample, a XRD pole figure scan was done oriented on the (200) peak because it was most intense. The pole figure probes (200) grain orientations looking for peaks from different phases. This pole figure, however, showed no features, indicating that the sample was not primarily (200) oriented. A likely explanation is that these samples have a few different preferred grains. Perhaps (200), (220), (112), (212), and (041) oriented grains formed, but others did not. The pole figure did not show any features, but it is also known that the grains are not completely random, so only a few of the preferred peaks show up on the 2θ scan. The grazing incidence scans and pole figures did not provide a clear explanation for this phenomenon, and lack of time and specialized equipment prevented further study.

4.2.7 Summary of PtSi XRD Data

Summary of PtSi XRD Data (Same color means similar XRD pattern)		
Samples:	Temperature sample was heated to before XRD spectrum was taken	Description of XRD pattern (Light blue=most uniform samples)
01_05 sample grown at 320C	Grown at 320°C	2 PtSi, 3 Pt2Si peaks (wide and low intensity peaks)
	Grown at 320°C Heated to 500/600/800°C	11 PtSi peaks (strong 200, 220 peaks)
	Grown at 320°C Heated to 500/600/800°C	Grazing incidence scan: 13 PtSi peaks (strong 200, 220 peaks)
01_10 sample grown at 320C	Grown at 320°C	9 PtSi peaks (strong 101 peak), 5 Pt2Si peaks
	Grown at 320°C Heated up to 850°C in N2 and 400°C in air	20 PtSi peaks (strong 101 peak), 14 Pt2Si peaks
01_24 grown at 0C	Grown at 0°C	7 PtSi peaks, 3 Pt2Si peaks
	Grown at 0°C Heated to 500/600/800°C	17 PtSi peaks, 7 Pt2Si peaks
	Grown at 0°C Heated to 1000°C	42 peaks with some PtSi, some Pt2Si, some langasite peaks present
02_16 grown at 400C	Grown at 400°C	7 PtSi peaks (strong 200, 220 peaks)
	Grown at 400°C Heated to 600°C	7 PtSi peaks (strong 200, 220 peaks)
	Grown at 400°C Heated to 800°C	14 PtSi peaks, 5 Pt2Si peaks
	Grown at 400°C Heated to 600°C then 800°C	14 PtSi peaks, 5 Pt2Si peaks
03_16 grown at 400C	Grown at 400°C	16 PtSi peaks (medium 101 peak)
	Grown at 400°C Heated to 500/600/800°C	16 PtSi peaks (medium 101 peak)
03_16 grown at 320C	Grown at 320°C	16 PtSi peaks (medium 101 peak)
	Grown at 320°C Heated to 500/600/800°C	16 PtSi peaks (medium 101 peak)

Figure 33. Summary of PtSi XRD data highlighting the similarities between samples.

PtSi grown between 300°C and 400°C then heated to 500°C and 600°C formed single phase PtSi without Pt_2Si present, while growing at lower temperatures or heating too quickly to 800°C caused Pt_2Si to form causing non-uniformity in the samples. While variation plagued the depositions, two samples had XRD spectra with very few PtSi peaks indicating more oriented grains. These samples are intriguing due to their higher level of organization causing further uniformity throughout the crystal. Other samples, prepared in the same exact way, had different PtSi peak intensities, and five more peaks, however they exhibited the same lack of Pt_2Si and the same thermal stability. Variability

in the deposition rates was a problem that plagued this set of experiments and could have caused samples to form different structures when prepared on different days.

An explanation for the formation of Pt_2Si with certain heat treatments, and lack of Pt_2Si in others can be postulated from an understanding of the typical platinum-silicon reaction pathway. When platinum is deposited on silicon, typically the platinum starts to react with silicon to form Pt_2Si, then later the excess silicon reacts with the Pt_2Si to form a PtSi crystal structure [29], [30]. The Pt_2Si reaction happens around 200°C while the PtSi reaction happens around 300°C or 350°C [31]. This process could explain the presence of Pt_2Si in samples grown at room temperature but not in samples grown at 320°C or 400°C after further heating. When grown at higher temperatures, the samples, which are co-deposited, can immediately start to form a PtSi structure, skipping the Pt_2Si phase. It could also explain how samples heated straight to 800°C still had Pt_2Si present, but samples that lingered between 500°C and 600°C had just the PtSi phase. Because the reaction between silicon and platinum happens faster at higher temperatures [32], samples heated directly to 800°C can become locked into a Pt_2Si+PtSi structure. When heating too fast, the Pt_2Si and PtSi reactions take place quickly and block remaining silicon from diffusing through the film to react with the remaining Pt_2Si. When lingering at lower temperatures, however, the reaction happens more slowly allowing time for all the Pt_2Si to react.

4.3 Studies of Pt_xSi_{1-x} Film Interactions with a Copper Overlayer

Due to equipment for sputtering a copper film on top of the PtSi not being available, only a few experiments were done to observe the interactions between copper and the PtSi films. In the time available, three samples were made: 500 nm of copper was sputter deposited on top of $Pt_{25}Si_7$ grown at room temperature, PtSi grown at 320°C, and PtSi grown at 400°C. The samples grown at 320°C and 400°C had the same crystal structure throughout this experimentation. When copper was added, the XRD pattern showed the original PtSi peaks with four added pure copper peaks as shown in Figure 34. After heating to 600°C, however, the sample changed completely as shown in Figure 35.

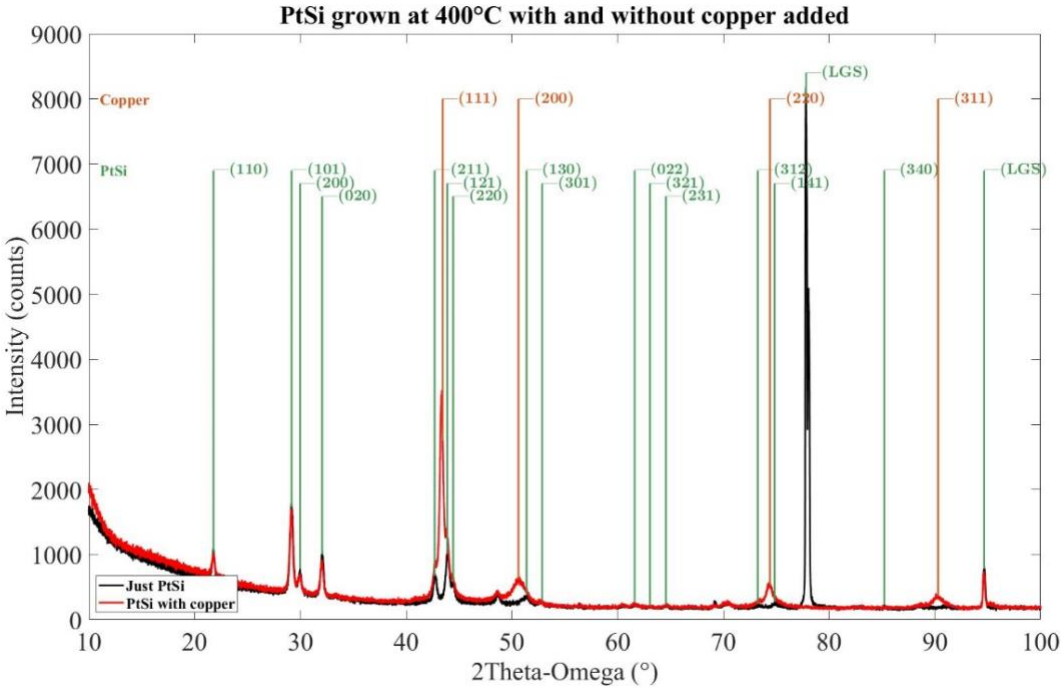

Figure 34. XRD spectra comparing PtSi grown at 400°C before and after 500nm of copper was added. Before, the sample is just a single phase PtSi (0.1° error) crystal, and after copper is added, it has the same PtSi peaks along with Cu peaks. Phases identified from PDF (04-003-0990), (00-004-0836) [33].

The PtSi peaks disappear, indicating that the PtSi reacted with the copper as there are no pure Pt, pure Si, or any platinum-silicon alloy peaks present in the XRD spectrum. The peaks present are not identifiable as any currently recognized Cu-Si or Cu-Pt alloy. The

copper also appears to crystallize into a (220) preferred orientation because the (111) copper peak loses intensity and the (220) increases in intensity. The XRD pattern, and therefore crystal structure was unchanged after another heat treatment this time to 800°C.

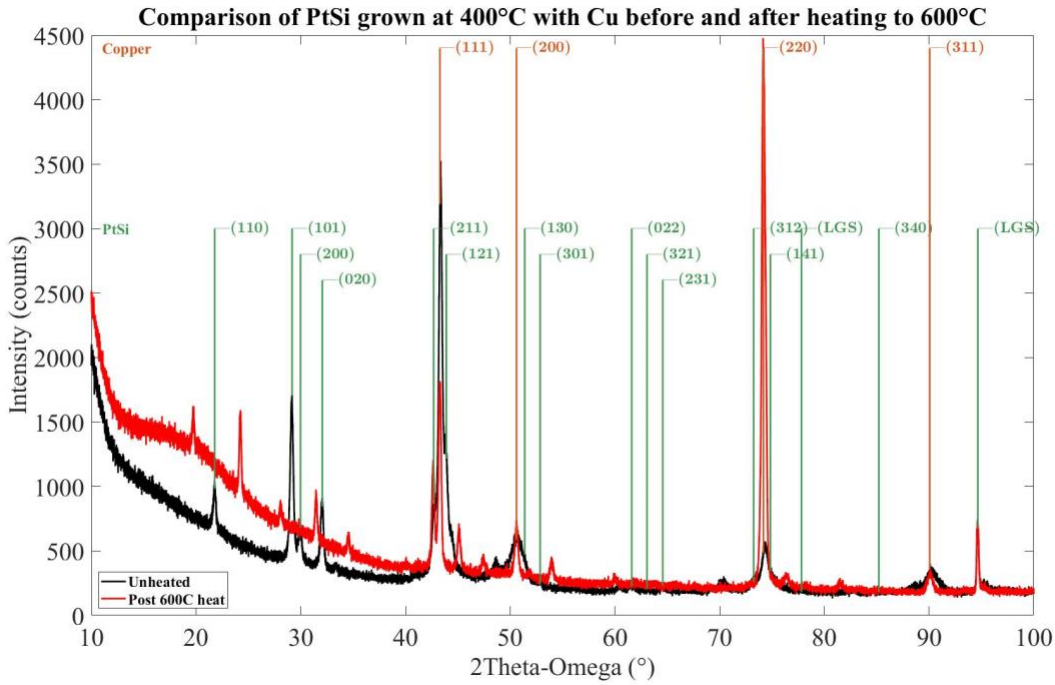

Figure 35. XRD spectra from PtSi grown at 400°C with Cu added before and after heating to 600°C in N_2. After heating, there is no sign of the PtSi alloy present, the Cu peak intensities change, and new, unidentified peaks appear. Phases identified from PDF (04-003-0990), (00-004-0836) [33].

While having some XRD peaks being unidentified makes it unclear exactly what happened, the PtSi peaks disappearing indicate a Pt/Si/Cu reaction takes place. The film that was created was thermally stable up to 800°C after previous cycling to 600°C, did not show any signs of cracking the langasite, and had a much more uniform crystal structure than that of previous experiments as shown in Figure 3. Future work will need to be done to attach the PtSi layer to copper. However, this preliminary work shows more promise than previous experiments with LGS and copper, which all ended in langasite cracking or very non-uniform bonding resulting in low adhesion strength.

The $Pt_{25}Si_7$ sample with copper added also just resulted in the addition of four copper peaks as shown in Figure 36. After heating to 600°C all the copper peaks and PtSi peaks disappeared, being replaced with unidentified peaks that did not fit any known Pt, Si, and Cu crystal structures as shown in Figure 37. This newly formed structure was unchanged after heating to 800°C. The films also had a grey appearance like many of the cracked LGS samples after heating in vacuum instead of having a copper color like the PtSi samples.

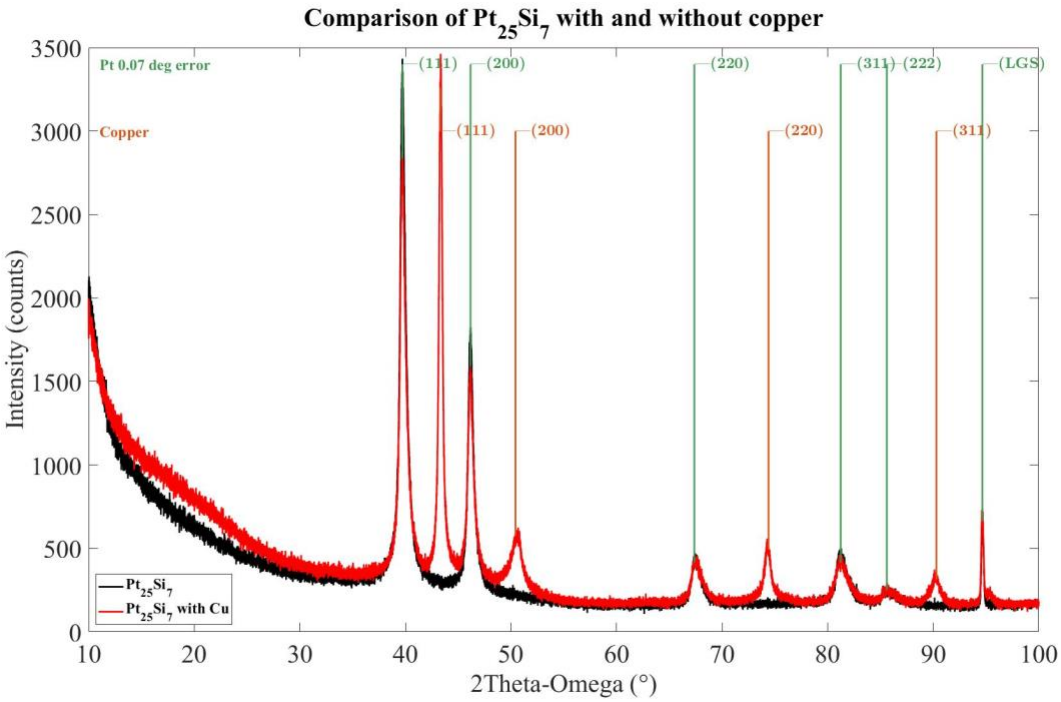

Figure 36. XRD spectra comparing $Pt_{25}Si_7$ grown at room temperature with and without copper added. Before the addition, Pt is the only crystal present and after Cu is added, the sample consists of pure Pt and pure Cu. Phases identified from PDF (00-004-0802), (00-004-0836) [33].

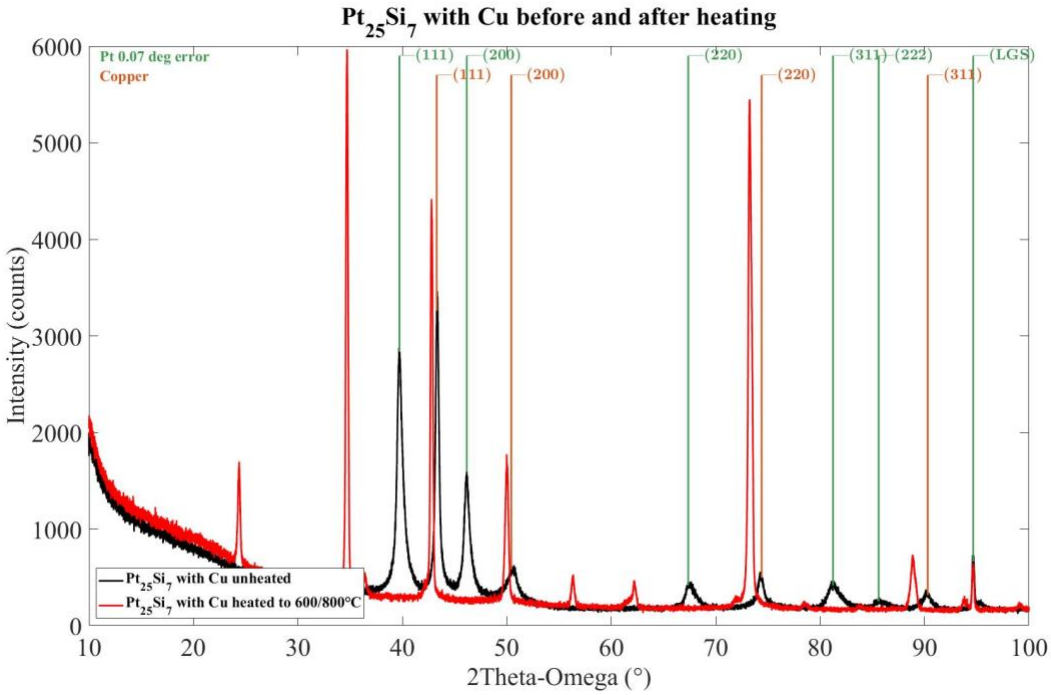

Figure 37. XRD spectra comparing $Pt_{25}Si_7$ grown at room temperature with copper before and after heating to 600°C. Before heating, pure Pt and Pure Cu crystal structures are present; after heating, only unidentified peaks are present. Phases identified from PDF (00-004-0802), (00-004-0836) [33].

5. CONCLUSIONS

Annealing treatments, including thermal cycling up to 800°C, have been found to have a strong influence on the crystal structure and thermal stability of Pt_xSi_{1-x} thin films grown on langasite using electron beam evaporation. For the film deposition conditions tested, PtSi films (1:1 Pt:Si ratio) deposited at a growth temperature of ~400°C followed by annealing up to 600°C for 10 minutes yields a single phase PtSi crystal structure that is thermally stable with uniform composition. The crystalline PtSi grains were found to be highly aligned along certain crystal planes, and the PtSi alloy composition was found to be very uniform. The PtSi samples prepared this way do not change with heating up to at least 850°C in nitrogen or 400°C in air and can withstand multiple thermal cycles without cracking. Adding a 500nm thick copper film on top of the PtSi films using a sputter deposition technique leads to a chemical reaction across the PtSi/Cu alloy interface upon annealing up to 800°C and the resulting structure shows promising stability for realizing strong interfacial adhesion with negligible cracking or delamination. The Cu/PtSi/langasite sample configuration investigated in this study has high promise for use in harsh environment microwave acoustic sensor technology.

6. FUTURE WORK

Deposition and annealing conditions which can form uniform, oriented, single phase PtSi structures on langasite that are thermally stable to 800°C were identified in this work. Experiments adding copper layers demonstrated uniformity and thermal stability. Future work should be done to refine the attachment of the PtSi layer to a copper layer. The copper layer is the next step in the multilayered adhesive identified in preliminary work [8]. The thin PtSi layer needs to be attached to a thin layer of copper and eventually to a bulk copper foil. Because copper interacts heavily with silicon, an experiment could be carried out to investigate the heating of a LGS/PtSi/100nmSi/200nmCu/bulk Cu multilayer structure. The proposed 100nm of silicon could help protect the PtSi layer from the copper and function as the intermediary. Experiments with thinner layers of sputtered copper could also reduce interaction with the PtSi layer. In this work, a PtSi/Cu reaction occurred which could be helpful in attaching langasite to bulk copper, but the XRD peaks were unidentifiable. Experimentation with different copper layers and added silicon should be performed to facilitate the adhesion between the identified PtSi layers and a copper layer. Copper can be attached well to steel [8], so attaching the identified stable PtSi film langasite to copper is the only necessary step for attaching langasite-based Surface Acoustic Wave Resonator strain sensors to steel.

During this project, strange phenomena occurred that were not addressed due to a limited amount of time. The lack of consistency between grazing incidence scans and pole figures on the oriented PtSi samples is something that should be investigated further. The grazing incidence and 2θ scans indicated an oriented film, but the pole figure showed only peaks from the langasite substrate. The working theory is that the PtSi films

were oriented primarily in multiple different directions instead of only one preferred orientation which could explain the lack of peaks on the pole figure. Further testing with specialized equipment and more time could reveal what is causing the discrepancy.

The reaction of langasite with tantalum that was identified during this project is also something worth exploring further. In the experiments, the langasite crystals often shattered, which is not ideal, but with refining the specific processing, this interaction could be used to attach langasite to tantalum. The CTE of tantalum is remarkably like that of langasite, so there is promise for successful adhesion that can withstand thermal cycling. As langasite does not melt until 1470°C, the reaction with the tantalum, which melts at almost 3000°C is unexpected. This clear evidence of a reaction, however, does indicate the possibility of an alternate method for attaching langasite to metals.

REFERENCES

[1] Ghosh, A., Zhang, C., Shi, S. Q., & Zhang, H. (2019). High-Temperature Gas Sensors for Harsh Environment Applications: A Review. *CLEAN – Soil, Air, Water, 47*(8), 1800491. https://doi.org/10.1002/clen.201800491

[2] Maskay, A., Hummels, D. M., & Pereira da Cunha, M. (2018). SAWR dynamic strain sensor detection mechanism for high-temperature harsh-environment wireless applications. *Measurement, 126*, 318–321. https://doi.org/10.1016/j.measurement.2018.05.073

[3] da Cunha, M. P. (2013). Wireless sensing in hostile environments. *2013 IEEE International Ultrasonics Symposium (IUS)*, 1337–1346. https://doi.org/10.1109/ULTSYM.2013.0342

[4] Pereira da Cunha, M., Lad, R. J., Davulis, P., Canabal, A., Moonlight, T., Moulzolf, S., Frankel, D. J., Pollard, T., McCann, D., Dudzik, E., Abedi, A., Hummels, D., & Bernhardt, G. (2011). Wireless acoustic wave sensors and systems for harsh environment applications. *2011 IEEE Topical Conference on Wireless Sensors and Sensor Networks*, 41–44. https://doi.org/10.1109/WISNET.2011.5725021

[5] *Langasite—Lanthanum Gallium Silicate (LGS)*. (n.d.). Retrieved March 26, 2023, from https://en.newpiezo.com/knowledge_base/1/langasite/

[6] Watanabe, A., Masuda, Y., & Omura, I. (2019). Infrared image correlation for thermal stress analysis of power devices. *Microelectronics Reliability, 100–101*, 113414. https://doi.org/10.1016/j.microrel.2019.113414

[7] Lutz, J., Schlangenotto, H., Scheuermann, U., & De Doncker, R. (2018). Packaging of Power Devices. In *Semiconductor Power Devices: Physics, Characteristics, Reliability* (pp. 427–488). Springer International Publishing. https://doi.org/10.1007/978-3-319-70917-8_11

[8] Kell Fremouw, Robert Lad (2022). Multi-Layered High Temperature Adhesive for Reliable Attachment of Wireless Langasite-Based Sensors to Steel Components.

[9] Sujan, D., Vincent, L., & Pok, Y. W. (2018). Material Selection for Interfacial Bond Layer in Electronic Packaging. *MATEC Web of Conferences, 202*, 01005. https://doi.org/10.1051/matecconf/201820201005

[10] Bernhardt, G., Silvestre, C., LeCursi, N., Moulzolf, S. C., Frankel, D. J., & Lad, R. J. (2001). Performance of Zr and Ti adhesion layers for bonding of platinum metallization to sapphire substrates. *Sensors and Actuators B: Chemical, 77*(1), 368–374. https://doi.org/10.1016/S0925-4005(01)00756-0

[11] Budhani, R. C., Prakash, H., Doerr, J., Bunshah, R. F. (1986). Summary Abstract:

Oxygen enhanced adhesion of platinum films deposited on thermally grown alumina surfaces. *Journal of Vacuum Science & Technology A: Vol 4, No 6*. (n.d.). https://avs.scitation.org/doi/10.1116/1.573619

[12] *Valence Band Control of Metal Silicide Films via Stoichiometry | The Journal of Physical Chemistry Letters*. (n.d.). Retrieved March 26, 2023, from https://pubs.acs.org/doi/10.1021/acs.jpclett.6b00799

[13] Sinha, A. K., Marcus, R. B., Sheng, T. T., & Haszko, S. E. (1972). Thermal stability of thin PtSi films on silicon substrates. *Journal of Applied Physics*, *43*(9), 3637–3643. https://doi.org/10.1063/1.1661781

[14] Chen, L. J. (2005). Metal silicides: An integral part of microelectronics. *JOM*, *57*(9), 24–30. https://doi.org/10.1007/s11837-005-0111-4

[15] Sellai, A., & Ouennoughi, Z. (2008). Analysis of frequency- and temperature-dependent interface states in PtSi/p-Si Schottky diodes. *Materials Science and Engineering: B*, *154–155*, 179–182. https://doi.org/10.1016/j.mseb.2008.09.048

[16] Fryer, R. T., & Lad, R. J. (2016). Synthesis and thermal stability of Pt3Si, Pt2Si, and PtSi films grown by e-beam co-evaporation. *Journal of Alloys and Compounds*, *682*, 216–224. https://doi.org/10.1016/j.jallcom.2016.04.260

[17] PhD, Fryer, R., & Lad, R. J. (2016). *Synthesis, Structure, and Thermal Stability of Electrically Conductive Co-Evaporated Pt(1-x)Si(x) Thin Films*, PhD thesis [The University of Maine]. https://digitalcommons.library.umaine.edu/etd/2544

[18] Gurylev, V., Wang, C. C., Hsueh, Y. C., & Perng, T. P. (2015). Growth of silica nanowires in vacuum. *CrystEngComm*, *17*(11), 2406–2412. https://doi.org/10.1039/C4CE02538E

[19] Kingzett, T. J., & Ladas, C. A. (1975). Effect of Oxidizing Ambients on Platinum Silicide Formation: I . Electron Microprobe Analysis. *Journal of The Electrochemical Society*, *122*(12), 1729. https://doi.org/10.1149/1.2134119

[20] Gadkari, P. R., Warren, A. P., Todi, R. M., Petrova, R. V., & Coffey, K. R. (2005). Comparison of the agglomeration behavior of thin metallic films on SiO2. *Journal of Vacuum Science & Technology A*, *23*(4), 1152–1161. https://doi.org/10.1116/1.1861943

[21] Galinski, H., Ryll, T., Elser, P., Rupp, J. L. M., Bieberle-Hütter, A., & Gauckler, L. J. (2010). Agglomeration of Pt thin films on dielectric substrates. *Physical Review B*, *82*(23), 235415. https://doi.org/10.1103/PhysRevB.82.235415

[22] Hong, S. Q., Hong, Q. Z., Li, J., & Mayer, J. W. (1994). Interdiffusion and reaction in Cu/PtSi/Si(100) systems. *Journal of Applied Physics*, *75*(8), 3959–3963. https://doi.org/10.1063/1.356016

[23] Chang, C. (1990). Reaction between Cu and PtSi with Cr, Ti, W, and C barrier layers.

Journal of Applied Physics, *67*(10), 6184–6188. https://doi.org/10.1063/1.345183

[24] Moulder, J. F., Stickle, W. F., Sobol, P. E., & Bomben, K. D. (1995). *Handbook of X-ray Photoelectron Spectroscopy: A reference book of standard spectra for identification and interpretation of Xps Data*. (J. Chastain, Ed.). Physical Electronics.

[25] *Vapor pressures of the Chemical Elements, vapor pressure of metals and halogens from –150 degrees C to 3500 degrees C including lead, aluminum, zinc, iodine, copper, indium, iodine, magnesium, selenium, lithium, iron, sodium and gallium*. (n.d.). Retrieved 2023, from https://www.powerstream.com/vapor-pressure.htm

[26] Tanner, L. E., & Okamoto, H. (1991). The Pt-Si (Platinum-Silicon) system. *Journal of Phase Equilibria*, *12*(5), 571–574. https://doi.org/10.1007/BF02645072

[27] *Tantalum—Thermal Properties—Melting Point—Thermal Conductivity—Expansion*. (2020, November 1). Material Properties. https://material-properties.org/tantalum-thermal-properties-melting-point-thermal-conductivity-expansion/

[28] Streller, F., Agarwal, R., Mangolini, F., & Carpick, R. W. (2015). Novel Metal Silicide Thin Films by Design via Controlled Solid-State Diffusion. *Chemistry of Materials*, *27*(12), 4247–4253. https://doi.org/10.1021/acs.chemmater.5b01413

[29] Abbes, O., Hoummada, K., Mangelinck, D., & Carron, V. (2013). Formation of Pt silicide on doped Si: Kinetics and stress. *Thin Solid Films*, *542*, 174–179. https://doi.org/10.1016/j.tsf.2013.07.023

[30] Larrieu, G., Dubois, E., Wallart, X., Baie, X., & Katcki, J. (2003). Formation of platinum-based silicide contacts: Kinetics, stoichiometry, and current drive capabilities. *Journal of Applied Physics*, *94*(12), 7801–7810. https://doi.org/10.1063/1.1605817

[31] Čechal, J., & Šikola, T. (2006). A study of the formation and oxidation of PtSi by SR–PES. *Surface Science*, *600*(20), 4717–4722. https://doi.org/10.1016/j.susc.2006.07.041

[32] Franco, N., Klepeis, J. E., Bostedt, C., Van Buuren, T., Heske, C., Pankratov, O., & Terminello, L. J. (2001). Valence band study of the PtSi by synchrotron radiation photoelectron spectroscopy. *Journal of Electron Spectroscopy and Related Phenomena*, *114–116*, 1191–1196. https://doi.org/10.1016/S0368-2048(00)00431-X

[33] International Centre for Diffraction Data, Powder Diffraction Files https://www.icdd.com/pdf-4-web/

AUTHOR'S BIOGRAPHY

Kell Fremouw was born in Seattle, Washington on May 11th, 2001. He moved to Orono, Maine in 2004 where he grew up walking his dog in the Maine woods, playing hockey, and hiking in Acadia National Park. In high school, he started kayaking and canoeing competitively and qualified for the ICF Junior Wildwater World Championships in Austria in 2017 and in Bosnia and Herzegovina in 2019. Kell graduated from Orono High School in 2019. During his time at the University of Maine he continued kayaking, qualifying for the Senior Wildwater World Championships in 2020 but also started participating in STEM outreach, tutoring, and became a physics TA. He received a NSF Research Experience for Undergraduates (REU) fellowship in Sensor Science and Engineering to carry out research in FIRST during the summer of 2022. Kell will complete his Engineering Physics degree in the spring of 2023. After graduation he will start his PhD program in Materials Science and Engineering at the University of Colorado in Boulder improving the durability and efficiency of perovskite solar panels.